waste

MDPI

Review

Innovative Techniques for Electrolytic Manganese Residue Utilization: A Review

Andrews Larbi [1,2], Xiping Chen [1,2,*], Suliman Muhammad Khan [1,2] and Tang Fangheng [1,2]

[1] School of Material Science and Engineering, Zhengzhou University, Zhengzhou 450001, China; alarbi@gs.zzu.edu.cn (A.L.); sulimankhan@gs.zzu.edu.cn (S.M.K.); fanghengtang@gs.zzu.edu.cn (T.F.)
[2] National and Local Joint Engineering Research Center for Green Mineral Metallurgy and Processing, Zhengzhou University, Zhengzhou 450001, China
* Correspondence: chenxiping@zzu.edu.cn

Abstract: Electrolytic Manganese Residue (EMR) is a secondary material generated during the process of manganese production, poses significant environmental challenges, including land consumption and contamination threats to soil and water bodies due to its heavy metal content, soluble manganese, ammonia nitrogen, and disposal issues. This review thoroughly examines EMR, emphasizing its metallurgical principles, environmental impacts, and sustainable treatment methods. We critically analyze various approaches for EMR management, including resource recovery, utilization of construction materials, and advanced treatment techniques to mitigate its environmental challenges. Through an extensive review of recent EMR-related literature and case studies, we highlight innovative strategies for EMR valorization, such as the extraction of valuable metals, conversion into supplementary cementitious materials, and its application in environmental remediation. Our findings suggest that integrating metallurgical principles with environmental engineering practices can unlock EMR's potential as a resource, contributing to the circular economy and reducing the environmental hazards associated with its disposal. This study aims to deepen the understanding of EMR's comprehensive utilization, offering insights into future research directions and practical applications for achieving sustainable management of electrolytic manganese waste. Finally, we propose some recommendations to address the issue of EMR, intending to offer guidance for the proper disposal and effective exploitation of EMR.

Keywords: resource utilization; electrolytic manganese residue; metallurgical principles; sustainable treatment; environmental impact

Citation: Larbi, A.; Chen, X.; Khan, S.M.; Fangheng, T. Innovative Techniques for Electrolytic Manganese Residue Utilization: A Review. *Waste* **2024**, *2*, 354–381. https://doi.org/10.3390/waste2030020

Academic Editor: Srecko Stopic

Received: 31 May 2024
Revised: 5 August 2024
Accepted: 6 August 2024
Published: 30 August 2024

1. Introduction

The mining and metallurgical industries have long played vital roles in driving global economic growth by supplying fundamental raw materials essential for a wide array of industrial applications [1,2]. One such crucial metal is manganese, which is extensively used in producing steel, alloys, batteries, and many other products critical to modern society [3,4]. The extraction of manganese through electrolytic processes has yielded remarkable strides in enhancing the efficiency of manganese production, thereby meeting the escalating demand for this versatile metal [5,6]. However, alongside the benefits of electrolytic manganese production, an equally significant challenge has emerged by generating substantial quantities of EMR [7,8]. Electrolytic manganese residue, often considered industrial waste, comprises various by-products and impurities from electrolytic manganese production [9]. Its disposal poses significant environmental and economic concerns. The disposal of EMRs into landfills consumes valuable land and raises the specter of soil and groundwater contamination due to heavy metals, such as manganese, cobalt, and nickel [10]. Moreover, the incineration of EMR releases harmful pollutants into the atmosphere, further contributing to environmental degradation [11,12].

To address these challenges and tap into the unexplored potential of EMR, researchers and metallurgists have increasingly turned their attention to the application of metallurgical principles in its recovery process. The recovery of valuable metals and converting waste into valuable resources align with the broader goals of sustainable development and the circular economy [13]. More so, to achieve a comprehensive understanding and maximize the utilization of EMR, it is imperative to delve into the chemical reactions of the process and conduct thermodynamic calculations. This approach is crucial for uncovering the underlying principles and energy dynamics involved. Therefore, this literature review explores the multifaceted dimensions of the application of metallurgical principles in the recovery process of EMR.

This paper aims to explore and review in detail the phase transformation of the EMR recovering process, coupled with thermodynamic analysis, to provide a comprehensive understanding of the principles and energy dynamics involved in harnessing the potential of EMR. By examining existing papers and case studies, this review shows the research status of comprehensive utilization of EMR, which are summarized and compared, hoping to deepen the understanding of other researchers and readers in the future. Subsequently, the authors proposed their remediation to address the EMR issue, intending to facilitate the extensive use of EMR.

1.1. The Electrolytic Manganese Metal Production

Electrolytic manganese metal (EMM) production is dominated by China, which accounts for more than 98% of the entire output on an annual basis [14–16]. However, this significant production has led to substantial environmental harm, primarily due to EMR [17,18]. EMR contains various pollutants such as NH_4^+-N, Mn, Mg, soluble sulfate, SeO_2, and heavy metals. Improperly managed EMR stockpiles, often exposed to the open air, result in severe ecosystem pollution, endangering nearby residents' health and well-being. Additionally, to ensure the sustainability of the EMM industry and support societal development, adopting more sustainable approaches for EMR treatment and disposal is imperative. Figure 1 depicts the effects of EMR on wildlife and ecosystems.

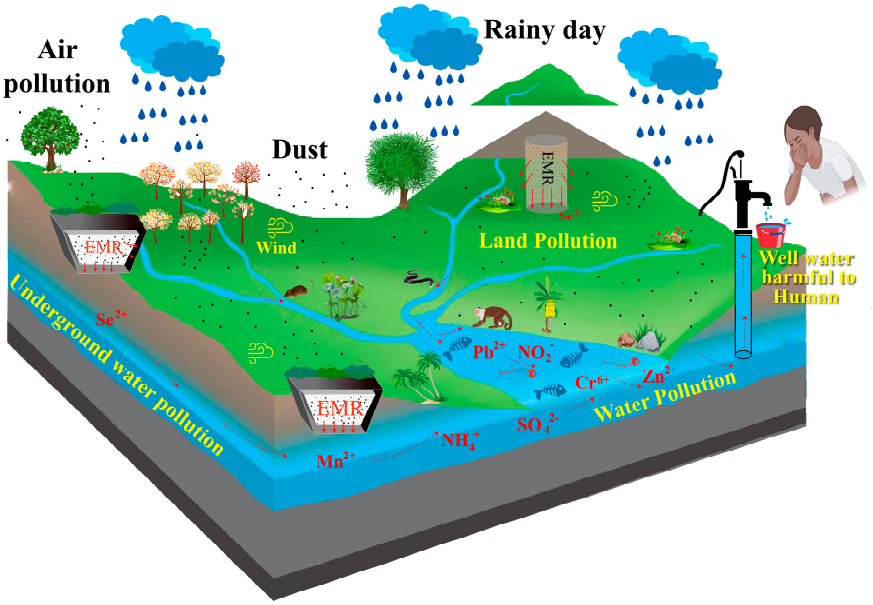

Figure 1. Illustration depicting the impact of EMR on ecological and animal life.

In significant countries that produce EMM, the stockpiling of EMR is carried out informally, with the selection of ditches, mountains, and other areas at lower elevations (Figure 1). Due to inadequate protection measures and planning, EMR can contaminate nearby water bodies and the environment, leading to significant infection and degradation

(Figure 1). At the same time, dam failures have occurred intermittently, affecting vast areas of agricultural land and causing numerous fatalities [19].

Manganese and its derivatives are widely used in various industries, including metallurgy, battery production, fertilizer manufacturing, chemical processing, pharmaceuticals, and especially in the steel sector [3,20]. The use of manganese metal constitutes more than 90% of the overall demand for manganese [21,22]. Incorporating manganese into steel significantly boosts its strength, resilience, and hardness, typically in amounts varying from 0.3 wt.% to 0.8 wt.% [13]. Electrochemical processes, electro-silicon thermal methods, and electrothermal methods can be used to extract manganese [13,23–25]. The electrolytic method is widely implemented in South Africa and China [26].

EMM production relies on raw materials such as rhodochrosite and pyrolusite. In South Africa, MMC utilizes high-quality pyrolusite in a process involving rotary kiln reduction roasting, followed by the use of H_2SO_4 solution to prepare $MnSO_4$ after roasting and SO_2 as an antioxidant during electrolysis [2]. This approach contrasts with China's EMM production, lowering pollution levels [15]. In China, rhodochrosite is the primary raw material used in this process. According to GB 3714-2017 standards, the manganese (Mn) content of rhodochrosite used must not be less than 18 wt.% [27]; however, recent technological advancements have facilitated the widespread adoption of rhodochrosite with manganese content ranging from 15% to 17% by weight in contemporary EMM [28]. The production of EMM encompasses several pivotal stages: (a) Sulfuric acid leaching, which initiates the dissolution of manganese-containing ores; (b) Iron removal through oxidation, a crucial step aimed at eliminating iron impurities from the leach solution; (c) Removal of heavy metals via vulcanized precipitation, which involves the precipitation of heavy metal impurities for subsequent removal; (d) Sedimentation settling, facilitating the separation of precipitates and allowing for further purification; and (e) The electrolysis process, where purified manganese sulfate solution undergoes electrolysis to yield high-purity electrolytic manganese metal [29]. Each of these steps plays a critical role in ensuring the efficiency and quality of the EMM production process.

1.2. Electrolytic Manganese Residue

In the manufacturing process of EMM, the term "EMR" commonly refers to the residual material produced during sulfuric acid leaching, oxidation for iron (Fe) removal, and subsequent sedimentation processes [16,30]. EMR is classified as a type of acid residue, which may be described as a black mushy powder substance with small particles, non-magnetic and water-insoluble. The pH level of EMR typically falls within the range of 5.0–6.5, with a moisture content ranging from 25% to 35% by weight when newly generated and particle sizes ranging from 20–500 mm [15].

Figure 2 illustrates the microstructure of EMR [31]. This structure predominantly consists of columnar and massive mineral particles intermingled randomly. Additionally, spherical minerals can be observed adorning the surfaces of these columnar structures through the application of energy-dispersive X-ray spectroscopy mapping and XRD analysis. Deng et al. [32] established that these columnar particles are primarily composed of $CaSO_4{\cdot}2H_2O$, while the spherical minerals predominantly consist of SiO_2, ferromanganese compounds, and ammonia nitrogen salts. Parallel findings have been reported in other research studies [14,33,34], which corroborate these observations. Over time, as EMR is stored, its microstructure featuring block, columnar, and spherical particles becomes denser. Throughout the storage period, elements like Mn undergo oxidation or carbonization into MnO or $MnCO_3$, respectively, and adhere to the surfaces of other particles [35].

Moreover, the particle size of EMR can vary depending on the time it has been stockpiled and the production procedure used [36,37]. Following the onset of precipitation, it solidifies and grows to enormous proportions. Table 1 depicts the physical characteristics of EMR [38]. The primary minerals present in EMR are quartz, gypsum, hematite, and ruizite, as depicted in Figure 2 [37]. The primary chemical constituents of EMR are aluminum oxide (Al_2O_3), calcium oxide (CaO), silicon dioxide (SiO_2), and sulfur trioxide (SO_3) [38,39].

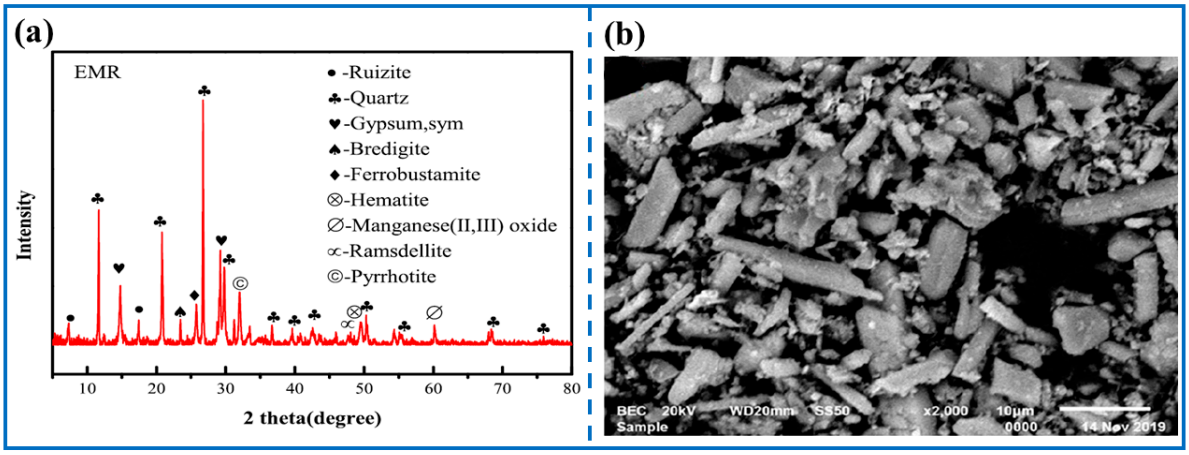

Figure 2. Illustrates the EMR's morphology: (**a**) XRD patterns and (**b**) SEM image referred from [31].

Table 1. The physicochemical characteristics of EMR [38].

Chemical Properties	Mass Fraction (%)	Physical Properties	Value
SiO_2	25–40	Density (g/cm^3)	2–3
Al_2O_3	8–20	Fineness (cm^2/g)	~3000
SO_3	20–30	Water content (%)	20–30
CaO	10	LOI (%)	~20
Fe_2O_3	5–10	average particle size (µm)	15–17
Mn^{2+}(EQV:MnO_2)	2–7	pH	4–6
MgO	1–3		

Note: LOI (%) is Loss on Ignition of the EMR.

2. Research Methodology

In this literature review, a comprehensive search for relevant sources was conducted using various reputable academic databases, such as Google Scholar, Web of Science, Scopus, ScienceDirect, American Chemical Society, Chinese publication site, and SpringerLink was widely utilized. The search aimed to include studies and articles published within the past 16 years (2008–2024) to ensure the relevance of the findings. The following are the primary procedures for selecting and analyzing relevant literature: (a) Search Strategy: A combination of appropriate keywords and phrases was used to retrieve articles. The search terms included "electrolytic manganese residue," "EMR recovery", "metallurgical principles", "pyrometallurgy", "hydrometallurgy", "manganese recovery", and related variations. Boolean operators (AND, OR) were employed to refine the search results. (b) During the screening process, the literature gathered is evaluated to exclude research publications irrelevant to the industrial production of EMM and EMR, lack clarity in their study findings, or possess less trustworthy recorded data. (c) Categorization: in this step, the selected works of literature were first categorized according to the objective of recovery EMR. Next, each category was then categorized according to phase transformation, treatment techniques, and product types obtained.

The literature is then summarized and assessed in depth based on assessment criteria such as the recovery ratio of EMR, chemical reactions and thermodynamic analyses, process operability, and industrial utilization prospects. Ethical guidelines for academic research and citation were followed throughout the review process. Proper citation practices were employed to give credit to the original authors and avoid plagiarism.

Furthermore, a brief bibliometric analysis was conducted utilizing the Scopus database to assess the present and past developments in EMR research. Bibliometric methods consist predominantly of various statistical techniques for counting bibliographies to evaluate and quantify the growth of literature within a specific field [40]. Bibliometric analysis is a

highly informative approach that provides insights into research publications' quantitative trends and historical developments about a specific topic [41]. The rationale for utilizing the Scopus database is its considerably greater abstract and citation coverage compared to other databases of a similar nature [42]. The database comprises more than 22,700 peer-reviewed indexed periodicals, facilitating a more extensive analysis encompassing a comprehensive range of aspects.

From the brief bibliometric analysis, the article [43] on Figure 3 holds the highest citation count among all influential works. This particular contribution was instrumental in establishing the foundation for the application of EMR in developing sustainable environments. China has emerged as the foremost contributor to scientific production in EMR research. Following behind are India, the United States, Australia, South Africa, and several other nations (Figure 4). The Figure 4 shows the global participation and diverse geographical distribution of research efforts in EMR.

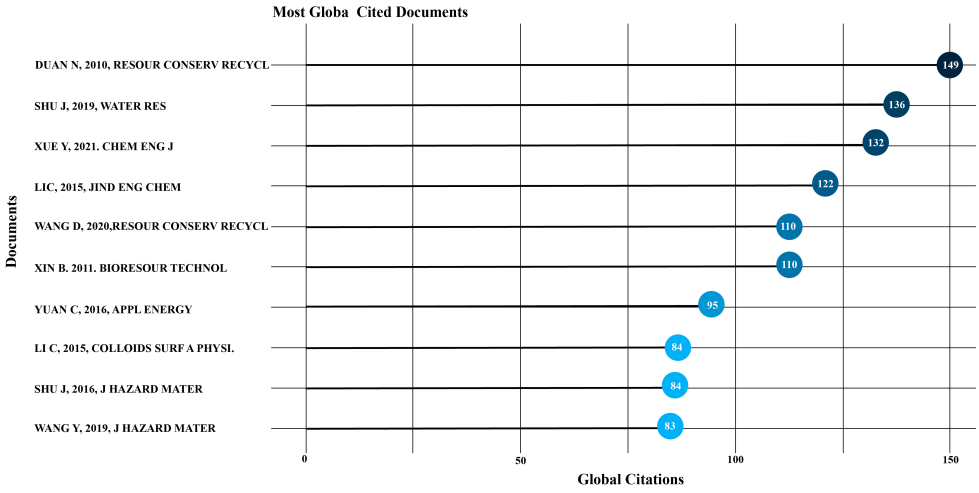

Figure 3. EMR Bibliometric data from SCOPUS: the ten most globally cited documents related to the use of EMR analyzed using Rstudio.

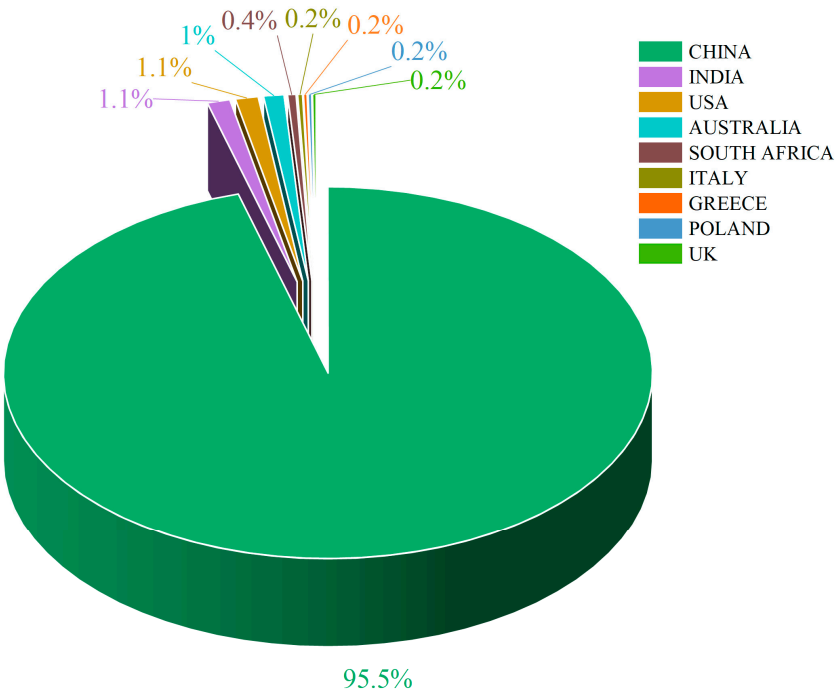

Figure 4. EMR Bibliometric data from SCOPUS: Proportional distribution of single countries production.

Conducting a comprehensive examination and documentation of the countries engaged in this research initiative can assist emerging scientists. This information serves as a foundation for forging scientific partnerships, launching joint projects, and exchanging inventive methods and concepts. Scholars from nations keen on advancing research in EMR can establish collaborations with subject matter experts, thereby gaining valuable insights and knowledge to enhance their contributions to the field of EMR.

3. Methods of Recovering Valuable Elements from EMR

As the metallurgical sector progresses and management and control technologies advance, the diminishing availability of mineral reserves and the reduction in related element grades have emerged as significant challenges. In light of this, increasing attention is being paid to exploring innovative approaches for sustainable development. Among these approaches is the exploration of deep extraction and recovery methods for valuable elements found within associated tailings, industrial by-products, and urban solid wastes [44]. This strategic shift aims to optimize resource utilization while mitigating environmental concerns, marking a pivotal step towards sustainable practices in the industry. EMR constitutes the principal solid waste produced by EMM operations. As per findings by Tian et al. [10], EMR typically comprises approximately 4–6 wt.% manganese, 3–4 wt.% ammonium nitrogen, 2–17 wt.% iron, and 11–20 wt.% silicon. Notably, these components exhibit significant potential for recycling, highlighting the importance of exploring efficient recycling strategies to harness their inherent value and contribute to sustainable resource management practices in the metallurgical industry. Therefore, various methods for recovering valuable elements of EMR and its related chemical reactions are vital to explore. Table 2 depicts a summary of commonly used chemical reagents in processes of EMR recovery.

Table 2. Summary of commonly used chemical reagents in processes of EMR recovery.

References	Leaching Reagent	Experimental Conditions	Recovery Efficiency
[45]	Pure Water	Roasting at low temperature (600 °C) for 60 min, water washing process at 25 °C with a S:L ratio of 1:4	Mn^{2+} recovery below 0.005 g/L
[46]	Pure Water	Ball milling with S:L ratio of 1:2, rotation at 250 rpm, volume ratio of electromagnet rotor to balls (VEMR/Vballs) of 0.8, fill factor of 0.12, duration of 30 min, and addition of oxalic acid dihydrate.	Mn^{2+} recovery at 98%, Fe below 2%, NH_4^+-N concentration at 13.65 mg/L
[47]	Pure Water	Leaching at 24 °C with a S:L ratio of 1:4 and an agitation rate of 300 rpm	Mn^{2+} recovery at 83.35%
[48]	Sulfuric Acid (H_2SO_4)	S:L = 1:4, temperature = 85 °C, H_2SO_4 concentration = 1.67 mol/L, $H_2C_2O_4$ concentration = 0.2mol/L, time = 120 min	Mn^{2+} recovery at 99.9%, Fe at 79.3%
[49]	Hydrochloric Acid (HCl)	S:L = 1:6, temperature = 100 °C, HCl concentration = 2 mol/L, time = 60 min	Recovery: Mn at 95.89%, Fe at 94.69%, Ca at 63.38%, Al at 2.21%, NH_4^+-N: 96.34%
[50]	NaOH	S:L = 1:5, temperature = 130 °C, NaOH concentration = 2 mol/L, time = 5 h, Stirring speed = 300 r/min	Si recovery at 82.04%
[51]	Nitric Acid (HNO_3)	S:L = 1:20, temperature = 50 °C, HNO_3 concentration = 2 mol/L, time = 2 h	Mn approach 100%

3.1. Water-Leaching

Water-leaching techniques are vital for improving the environmental safety of EMR by more effectively reducing the concentration of harmful substances such as NH_4^+, Mn^{2+}, and

other heavy metals, making the residue safer for disposal or further processing [11]. Washing is effective for removing soluble Mn^{2+} and NH_4^+ from EMR, however, it demonstrates limited efficacy in removing insoluble substances [16,52]. Additionally, washing can disrupt water balance, potentially requiring additional investment to treat the resulting washing liquid. Zheng et al. [47] used water leaching to recover soluble manganese from EMR. They developed a kinetics model for the leaching process. They used leaching diffusion-controlled, with an activation energy of 11.17 ± 2.02 kJ/mol. Optimal leaching achieved 83.35% Mn recovery under specific conditions (S: L ratio of 1:4, 24 °C, 300 r/min agitation).

The study by Shu et al. [53] employed a strategic approach for the extraction of Mn^{2+} and the reduction of NH_4^+-N from EMR through a novel selective water leaching followed by electrooxidation. The technique facilitated the efficient recovery of manganese with over 98% efficiency. Their method was particularly effective in converting NH_4^+-N to ammonium sulfate. Mn was predominantly extracted through this process in MnO_2, Mn_2O_3, MnOOH, and Mn_3O_4. Also, NH_4^+-N was oxidized to N_2. As a result, the final concentrations of Mn^{2+} and NH_4^+-N meet the stringent requirements of the comprehensive wastewater discharge standards (GB 8978-1996) [54].

More so, Lan et al. [46] developed a method for the selective recovery of manganese and removing ammonium sulfate. By combining ball milling and adding oxalic acid, they achieved a manganese recovery rate exceeding 98% while maintaining an iron leaching rate below 2%. The process also reduced the leaching rates of Mn^{2+} and NH_4^+-N to 1.01 and 13.65 mg/L, respectively. Equation (1) depicts the method of manganese recovery rate.

$$\text{Manganese recovery } (\%) = \frac{C_0V_0 - C_1V_1}{C_0V_0} \times 100\% \quad (1)$$

where C_0 and C_1 represent the initial and final concentrations of manganese (mg/L), V_0 and V_1 represent the initial and final volumes of the manganese solution (L), respectively.

From their study, the reactions that occurred were the formation of Mn_3O_4, outlined in the equations below [46]:

$$Mn^{2+} + 2NH_3{\cdot}H_2O \leftrightarrow Mn(OH)_2 \downarrow + 2NH_4^+ \quad (2)$$

$$2Mn(OH)_2 + O_2 \leftrightarrow 2MnO(OH)_2 \quad (3)$$

$$MnO_2 + 4OH^- \leftrightarrow MnO_4^{4-} + 2H_2O \quad (4)$$

$$2Mn(OH)_2 + H_4MnO_4 \leftrightarrow Mn_3O_4 + 4H_2O \quad (5)$$

$$Mn^{2+} + 2NH_3{\cdot}H_2O + CO_2 \leftrightarrow MnCO_3 \downarrow + 2NH_4^+ + H_2O \quad (6)$$

He et al. [45] revolutionized the treatment of EMR by employing a low-temperature roasting-water washing technique, achieving a manganese recovery rate of 67.12% with roasting at 600 °C for 60 min, followed by a 25-min deionized water washing. Their method enhanced manganese recovery and transformed unstable EMR phases into stable forms, ensuring the post-treatment residue met the Chinese Integrated Wastewater Discharge Standard GB 8978-1996. Their study revealed that the EMR sample's phase transformation features can be studied by roasting it at low temperatures in the air, which is a significant use of EMR. Detailed reactions of the process during the slow roasting procedure at low temperatures can be found in the study of [45]. More so, the utilization of oxalic acid in aqueous solutions facilitates pH adjustment and promotes Mn^{2+} leaching, contributing to efficient recovery processes. The response may be mainly in three parts:

$$MnO_2 + 2H_2C_2O_4 \xrightarrow{\Delta} MnC_2O_4 + 2CO_2 + 2H_2O \quad (7)$$

$$MnC_2O_4 \xrightarrow{\Delta} MnO + CO + CO_2 \quad (8)$$

$$MnO + 2H^+ \longrightarrow Mn^{2+} + H_2O \quad (9)$$

In summary, water-leaching techniques offer significant promise for improving the environmental safety and resource recovery potential of EMR [45]. These techniques have shown efficacy in reducing the concentration of harmful substances such as NH_4^+, Mn^{2+}, and other heavy metals, thereby making the residue safer for disposal or further processing. While traditional washing methods have demonstrated limited effectiveness in removing insoluble substances from EMR, water leaching has emerged as a more efficient alternative.

3.2. Chemical Leaching: Acid-Leaching

Acid-leaching is widely used in industrial fields like metal processing and the recovery of materials from waste. This method involves using acids, including nitric acid (HNO_3), hydrochloric acid (HCl), sulfuric acid (H_2SO_4), and various organic acids [55–57]. The purpose is to efficiently extract valuable metals and elements from ores and solid wastes. This technique is vital because it enables the recovery of valuable elements, which might otherwise be lost, and helps efficiently process metal ores. One standard method for treating EMR is acid leaching [58–60]. Chen et al. [48] used H_2SO_4 at a concentration of 1.67 mol/L and $H_2C_2O_4$ at 0.2 mol/L to leach EMR. The oxalic acid facilitated the conversion of insoluble manganese compounds in EMR into soluble divalent manganese, consequently enhancing the leaching efficiency of manganese. Following a reaction period of 120 min at 85 °C, the recovery rates for manganese and iron were nearly complete, with manganese reaching close to 100% recovery and iron achieving a recovery rate of 79.3%. Also, Rao et al. [61] used H_2SO_4 solution with galena as the reductant, and their result yielded a 98% leaching efficiency of Mn. Through NH_4Ac leaching followed by $(NH_4)_2CO_3$ precipitation, Pb was efficiently recovered, resulting in an 85% yield of the $PbCO_3$ product. The NH_4Ac leaching solution was regenerated successfully by eliminating the residual CO_3^{2-} and SO_4^{2-} ions. In a study by Yang et al. [49], EMR was leached at 100 °C for 60 min using HCl at a 2 mol/L concentration.

3.3. Leaching Mechanism

During the leaching process of EMR, two notable phenomena could be observed. Firstly, manganese observed to migrate from the surface of the EMR to the surrounding liquid for dissolution. Secondly, metal ions such as manganese, ammonia nitrogen, and irons present in the EMR can dissolve when subjected to acidic conditions. This phenomenon is illustrated by Equations (10)–(12) in the study conducted by [10].

$$Fe(OH)_3 + 3H^+ \rightarrow Fe^{3+} + 3H_2O. \quad (10)$$

$$Fe(OH)_2 + 2H^+ \rightarrow Fe^{2+} + 2H_2O. \quad (11)$$

$$Mn(OH)_2 + 2H^+ \rightarrow Mn^{2+} + 2H_2O. \quad (12)$$

Enhancements were observed in the leaching efficiencies of manganese, ammonia nitrogen, and heavy metals. The primary reactions contributing to these improvements are outlined below:

$$Mn^{3+} + Fe^{2+} \rightarrow Fe^{3+} + Mn^{2+} \quad (13)$$

$$MnO_2 + Fe^{2+} + 4H^+ \rightarrow Mn^{2+} + Fe^{3+} + 2H_2O \quad (14)$$

$$Fe^{3+} + e^- \rightarrow Fe^{2+} \quad (15)$$

$$H_2O_2 + Fe^{2+} \rightarrow Fe^{3+} + (OH)^- + OH \quad (16)$$

Mn^{2+}andNH_4^+ recovery.

In a study by Tian et al. [10], NaOH was used to adjust the leaching solution pH, and Na_2CO_3 was used to recover manganese, as well as $NaH_2PO_4{\cdot}2H_2O$ and $MgCl_2$ were used to recover ammonia nitrogen from the leaching solution. The reactions involved are as follows [10]:

$$Mn^{2+} + CO_3^{2-} \rightarrow MnCO_3 \downarrow K_{sp} = 9.0 \times 10^{-11} \quad (17)$$

$$Mg^{2+} + PO_4^{3-} + NH_4^+ + 6H_2O \rightarrow Mg(NH_4)PO_4{\cdot}6H_2O \downarrow \quad (18)$$

$$Mg^{2+} + H_2PO_4^- + NH_4{}^+ + 6H_2O \rightarrow Mg(NH_4)PO_4{\cdot}6H_2O \downarrow + 2H^+ \quad (19)$$

Electrochemical/Electric field extraction mechanism of EMR.

The electrochemical extraction of metals from EMR involves several vital processes, including leaching, reduction, and electrodeposition. Initially, EMR leaching is performed to dissolve metal species into a solution. This step is crucial for making metals accessible for subsequent electrochemical processes. Various types of manganese ions are present in the leaching solution of manganese residue, posing a challenge in their recovery. Additionally, the propensity of metal ions to undergo oxidation should be considered during the electrochemical treatment of electrolytic manganese residue [32,61–63]. The electrochemical principle involves studying the ammonia nitrogen content in manganese residue leaching solution by altering parameters such as the type of additives, voltage intensity, solid-to-liquid ratio, and other relevant conditions [60].

The electrochemical electrolysis extraction of manganese from EMR involves three main reactions, which can be classified into the following procedures:

(1) In the acidic system, Fe^{3+}/Fe^{2+} were extracted from EMR:

$$Fe^{3+} + 3H_2O \leftrightarrow Fe(OH)_3 + 3H^+ \quad (20)$$

$$Fe^{2+} + 2H_2O \leftrightarrow Fe(OH)_2 + 2H^+ \quad (21)$$

(2) At the anode, low-valent Mn^{2+} and Fe^{2+} compounds undergo direct oxidation. The primary reactions at the anode are outlined as follows:

$$2H_2O \leftrightarrow O_2 + 4H^+ + 2e \quad (22)$$

$$Mn^{2+} \leftrightarrow Mn^{3+} + e \quad (23)$$

$$Fe^{2+} \leftrightarrow Fe^{3+} + e \quad (24)$$

$$2H_2O + Mn^{2+} \leftrightarrow 4H^+ + MnO_2 + 2e \quad (25)$$

(3) The reactions on the cathode;

$$2H_2O + 2e \leftrightarrow H_2 \uparrow + 2OH^- \quad (26)$$

$$Fe^{3+} + e \leftrightarrow Fe^{2+} \quad (27)$$

$$H_2O + 1/2O_2 + e \leftrightarrow H_2O_2 \quad (28)$$

The overall reactions are as follows:

$$Mn^{3+} + Fe^{2+} \leftrightarrow Fe^{3+} + Mn^{2+} \quad (29)$$

$$MnO_2 + 2Fe^{2+} + 4H^+ \leftrightarrow Mn^{2+} + 2Fe^{3+} + 2H_2O \quad (30)$$

In the above reactions, an electric field can enhance the extraction efficiency as Fe^{3+} is reduced to Fe^{2+} at the cathode region. Consequently, the high valence of manganese in EMR can be reduced to Mn^{2+} by Fe^{2+}.

Shu et al. [64] investigated an enhanced electroreduction method for leaching manganese from the EMR. Manganese was leached at an optimal efficiency of 84.1% under 9.2% H_2SO_4, 25 mA/cm^2 current density, 1:5 solid-to-liquid ratio, and 1-h leaching duration. The results revealed that the leaching rate is 37.9% greater than the value obtained without an electric field. Meanwhile, EMR experienced a reduction in manganese content from 2.57% to 0.48%. In a study by Shu et al. [65], EMR was added to the acid-leaching solution. Then, they incorporated sodium dodecyl benzene sulfonate, citric acid, and EDTA in specific molar ratios. Subsequently, a pulsed electric field was applied to the mixture.

After 84 h, the highest removal rates achieved were 94.74% for manganese and 88.20% for ammonia nitrogen.

Shu et al. [23] introduced a solution containing 9.2 wt.% H_2SO_4 and $FeSO_4 \cdot 7H_2O$ to EMR, with a mass ratio of Mn to Fe^{2+} of 1. The presence of Fe^{2+} in the leaching solution converted high-value Mn to low-value Mn and enhanced the leaching rate of manganese. When an electric field was introduced to the mixture, the leaching rate of Mn reached 96.2% after 1 h. Tian et al. [10] employed a leaching solution of 9.15 wt.% H_2SO_4 and H_2O_2. Fe^{2+} catalyzed H_2O_2 to form OH in an acidic solution, greatly improving metal ion and NH_4^+-N leaching. At a current density of 35 mA/cm^2, Mn and NH4+-N leaching rates reached 88.07% and 91.50%, respectively, after 120 min at 40 °C. Additionally, Shu et al. [60] utilized 13 wt.% H_2SO_4 solution for leaching and employed an electric field for reinforcement. Their results show that, Mn leaching rate was 89.4% and NH_4^+-N leaching rate was 65.9% during a 120-min reaction at 20 °C. The leaching rates of Mn and NH_4^+-N were raised to 97.1% and 98.4%, respectively, when 100 mg/L of surfactant tetracylate trimethyl ammonium chloride was added to the leaching solution.

In summary, the accelerated leaching of EMR is attributed to the enrichment and transfer of Mn^{2+} and NH_4^+-N. However, this process necessitates electric field enhancers, consuming significant energy and generating excess electrolytes, as highlighted by Liu et al. [66]. Moreover, the addition of these enhancers poses potential risks of secondary pollution [66,67].

3.4. Alkaline-Leaching

The alkaline leaching method utilizes alkaline solutions, typically containing agents such as sodium hydroxide (NaOH) or calcium hydroxide ($Ca(OH)_2$), to selectively dissolve and extract metals like Mn and Mg from the waste residue [51,68]. For manganese recovery, alkaline leaching transforms manganese present in the residue into soluble manganese salts, facilitating their subsequent recovery from the leachate [69,70]. Similarly, magnesium, contributing to the magnesium hazard of EMR, can also be effectively managed and recovered through this process [71]. Moreover, alkaline leaching can immobilize ammonia and heavy metals, mitigating the environmental risks associated with EMR disposal [71,72]. Shu et al. [70] investigated the leaching behaviors of Mn^{2+} and NH_4^+-N from EMR across different pH conditions; the study revealed that alkaline leaching significantly reduces the release of these substances compared to acidic conditions. The study highlights the potential of alkaline leaching as an environmentally friendly approach for EMR management, reducing environmental impacts by minimizing heavy metal releases.

A study by Zhang et al. [73] developed a method for creating mesoporous silica from EMR slags using amino-ended hyperbranched polyamide (AEHPA) as a novel template. Their technique enhances mesoporous silica's structural properties, such as increased specific surface area, pore volume, and optimal pore diameter. Under the optimal synthesis condition utilizing 0.3 wt.% AEHPA-2, mesoporous silica was obtained, exhibiting a specific surface area of 451.34 m^2/g, pore volume of 0.824 cm^3/g, and a pore diameter of 7.09 nm.

More so, the primary reaction between EMR and NaOH solution in liquid-solid non-catalytic in heterogeneous reactions; the main chemical reactions and phase transitions that occur are as follows:

$$2NaOH_{(aq)} + nSiO_{2(s)} \leftrightarrow Na_2O \cdot nSiO_{2\ (aq)} + H_2O \quad (31)$$

$$Mn^{2+}_{(aq)} + 2OH^-_{(aq)} \leftrightarrow Mn\left(OH\right)_{2(s)} \downarrow \quad (32)$$

Although the reaction of NaOH and SiO_2 itself does not generate solid products because the solid-liquid separation cannot be realized entirely in the process of EMR pressure filtration, there is a phase when part of the electrolyte stock solution remains [50].

In summary, alkaline leaching presents a promising method for extracting and managing metals from EMR. Alkaline leaching offers environmental benefits by immobilizing ammonia and heavy metals, reducing potential risks associated with EMR disposal [72–74]. However, challenges such as energy consumption, excess electrolyte generation, and the

potential for secondary pollution limit the need for further research and optimization of this method to enhance its efficiency and sustainability in metal recovery and waste management practices.

3.5. Bioleaching

Bioleaching, a novel hydrometallurgical method, involves using microorganisms to extract elements from ores or waste materials. Compared to traditional physical and chemical processes, bioleaching offers substantial advantages such as simplicity, cost-effectiveness, and environmentally friendly operation [75,76]. The increasing attention towards this method can be attributed to its optimal reaction conditions, minimal equipment requirements, minimal investment costs, and high selectivity for target elements. These advantages are particularly evident in using industrial solid waste and residual resources. As a result, this method emerges as a compelling option for various applications, offering efficient extraction and sustainable solutions for resource management and waste utilization [77–79].

Various studies have explored the application of bioleaching technology in extracting elements from EMR, a type of industrial waste rich in valuable metals and minerals [76,80–82]. Xin et al. [83] investigated the use of pyrite-leaching bacteria and sulfur-oxidizing bacteria in bioleaching EMR, demonstrating that the combined action of these strains enhanced the leaching efficiency of manganese. The sulfur-oxidizing bacteria achieved a maximum extraction efficiency of 93% for Mn after nine days of bioleaching with a sulfur concentration of 4.0 g/L. The bacteria used for leaching pyrite demonstrated their peak effectiveness in extracting manganese, achieving a remarkable efficiency of 81%. This level of extraction was revealed when the concentration of pyrite in the aqueous solution was maintained at 4.0 g/L.

Lv et al. [84] focused on examining the impact of two bacterial species, Bacillus mucilaginosus and Bacillus circulans. Their research specifically targeted these bacteria' role in synthesizing EMR, focusing on activating silicon and stabilizing heavy metals. Their findings emphasized the importance of direct contact between bacteria and EMR for improved efficiency, leading to significant leaching of Si and stabilization of metal ion concentrations. Moreover, Lv et al. [85] utilized Paenibacillus mucilaginosus bacteria for Si bioleaching from EMR. Their research highlighted the differential effects of P. mucilaginosus on Si-containing minerals, demonstrating its potential for selective extraction. Duan et al. [86] utilized bacteria that oxidize sulfur and iron for the bioleaching of Mn from EMR. Their study revealed high leaching efficiency, especially when using a combination of both bacterial strains. Similarly, Lan et al. [75] isolated bacteria from EMR and utilized waste molasses as a carbon/nitrogen source for bioleaching EMR. They achieved impressive leaching efficiencies for sulfur, manganese, magnesium, iron, and ammonium ions, followed by recovering valuable compounds through pH adjustment.

Zhao et al. [77] investigated the bioleaching capabilities of a novel Penicillium oxalicum strain Z6-5-1, focusing on manganese Mn^{2+} recovery from EMR. Their study highlighted the strain's exceptional bioleaching performance, achieving a Mn^{2+} recovery rate of 93.3% within seven days, marking a significant improvement over previously reported fungal efficiencies in similar durations. The primary mechanisms identified for Mn bioleaching included the generation of bio-organic acids, with a notable emphasis on gluconic and oxalic acids, alongside mycelial adsorption. More so, the researchers discovered a novel transcription factor, PoxCxrE, within P. oxalicum, which plays a crucial role in regulating the biosynthesis of these acids.

Furthermore, it is noteworthy that the manganese residues exhibited a dual composition, consisting predominantly of soluble Mn^{2+} forms, such as $MnSO_4$, while also containing minor amounts of insoluble Mn^{4+} forms, like MnO_2. The bioleaching system, characterized by a lower pH due to the presence of sulfur, played a pivotal role in promoting the dissolution of soluble Mn^{2+} into the aqueous phase, thereby enhancing the efficiency of the process. Lan et al. [87] conducted a study to unravel the intricate mechanism behind the bio-leaching of Mn from EMR. Additionally, their research delved into exploring the

metabolic characteristics of a newly discovered microorganism, Macrobacterium trichothecenolyticum Y1, within a bio-leaching framework incorporating a blend of EMR and waste molasses, a residual product from the sugarcane industry. The chemical process can be delineated as follows: Firstly, it initiates with the leaching of soluble manganese, predominantly $MnSO_4$, from EMR. Secondly, follows with the leaching of insoluble manganese, mainly comprising MnO_2, from EMR: (Equations (34)–(36)) [87]:

$$MnO_2 + \frac{2}{z-2x-y}C_xH_yO_z + 2H^+ \xrightarrow{Y1} M^{2+} + \frac{2x}{z-2x-y}CO_2 + \frac{2z-4x}{z-2x-y}H_2O \quad (33)$$

$$Mn^{2+} + 6H_2O \rightarrow Mn(H_2O)_6^{2+} \quad (34)$$

$$Mn^{2+} + O_2 + H_2O \rightarrow MnO(OH)_2 \quad (35)$$

$$MnO(OH)_2 + \frac{2}{y-2z-4x}C_xH_yO_z + 2H^+ \xrightarrow{Y1} M^{2+} + \frac{2x}{y-2z-4x}CO_2 + \frac{3y-4z-8x}{y-2z-4x}H_2O \quad (36)$$

These investigations shed light on the dynamic interplay between EMR, microbial activity, and waste utilization, offering insights into potential applications in environmental remediation and sustainable resource management.

In summary, bioleaching offers a promising and eco-friendly method for extracting valuable elements from ores and waste materials. Its simplicity, cost-effectiveness, and high selectivity make it an attractive alternative to traditional methods. Studies on bioleaching, particularly in dealing with EMR, highlight its effectiveness in extracting manganese and stabilizing heavy metals. Novel bacterial strains like Penicillium oxalicum show impressive results in manganese recovery. Understanding the chemical processes involved sheds light on how bioleaching can contribute to environmental remediation and sustainable resource management.

3.6. Roasting

Roasting technology is pivotal in metallurgy, particularly in recovering essential elements from EMR [88]. This advanced extraction technique involves heating EMR at elevated temperatures with various chemical agents under controlled atmospheric conditions [89–91]. The process effectively transforms complex raw materials into more separable forms, facilitating the efficient extraction of target elements [91–93].

Peng et al. [94] developed a method to recover iron and manganese from EMR using a two-step roasting process followed by magnetic separation. Initially, the EMR underwent oxidative roasting in air and reductive roasting in a CO atmosphere. The optimal conditions identified for the process included roasting at 750 °C for 30 min under air and CO atmospheres. Magnetic separation was subsequently applied, using a weak magnetic field of 1000 G to recover iron, resulting in a concentrate grade of 62.21% and a strong magnetic field of 12,000 G for manganese recovery, yielding a concentrate grade of 35.21%. Their study successfully demonstrated that 72.29% of iron and 90.75% of manganese could be recovered from EMR, showcasing a promising method for recycling valuable metals from industrial waste.

Sun et al. [5] developed a clean production method for electrolytic manganese involving EMR calcination with 4.0 wt.% coke to reduce sulfur content for cement use and a novel five-stage countercurrent manganese oxide ore and anolyte (MOOA) desulfurization process to clean high SO_2-containing flue gas. Their results achieved 99.7% sulfur reutilization from EMR, producing a manganese product with 99.93% purity. This integrated approach significantly enhances the electrolytic manganese industry's environmental and resource efficiency. Here are the primary chemical reactions involved [5];

$$CaSO_4 + C \rightarrow CaO + SO_2 + CO \quad (37)$$

$$2C + O_2 \rightarrow 2CO \quad (38)$$

$$CaSO_4 + CO \rightarrow CaO + SO_2 + CO_2 \quad (39)$$

$$CaSO_4 + 2C \rightarrow CaS + 2CO_2 \quad (40)$$

$$CaSO_4 + 4CO \rightarrow CaS + 4CO_2 \quad (41)$$

$$3CaSO_4 + CaS \rightarrow 4CaO + 4SO_2 \quad (42)$$

The mechanisms for sulfur release during the process are outlined as follows: Initially, the introduced coke directly interacts with $CaSO_4$ (Equation (39)). Secondly, the coke is oxidized to produce CO, which reacts with $CaSO_4$ (Equations (40) and (41)). Although the reaction of $CaSO_4$ with carbon or CO results in the formation of CaS (Equations (41) and (42)), which can react with $CaSO_4$ at temperatures above 1200 °C, leading to its consumption [5].

The reaction ended with a reduction in the amount of MnO_2 present, accompanied by the production of H_2SO_4 (Equation (46)), which reacted with Mn_2O_3 to generate new MnO_2 (Equation (46)), with or without the aid of metallic ions (Mn^{2+} and Fe^{3+}, (Equation (45)) [95].

$$MnCO_3 + H_2SO_4 \rightarrow MnSO_4 + H_2O + CO_2 \quad (43)$$

$$MnO_2 + SO_2 \rightarrow MnSO_4 \quad (44)$$

$$SO_2 + O_2 + H_2O \xrightarrow{Mn^{2+}} H_2SO_4 \quad (45)$$

$$Mn_2O_3 + H_2SO_4 \rightarrow MnSO_4 + MnO_2 + H_2O \quad (46)$$

The study noted that the atomization and mixing conditions in the pilot-scale desulfurization process are suboptimal due to the limitations imposed by the size of the equipment. Therefore, in practical implementations, there is significant room for enhancing the efficiency of manganese leaching (Equations (47) and (48)) [95].

$$Mn_yO_x + 3y/2H_2SO_4 + yFeSO_4 \rightarrow yMnSO_4 + y/2Fe_2(SO_4)_3 + 3y/2H_2O \quad (47)$$

$$Mn_yO_x + (x-y)H_2O_2 + yH_2SO_4 + \rightarrow yMnSO_4 + xH_2O + (x-y)O_2 \quad (48)$$

Additionally, Huang et al. [96] introduced a low-temperature CaO roasting process for treating EMR, focusing on ammonia removal and the immobilization of manganese and magnesium. They optimized the process parameters, finding that a CaO: EMR ratio of 1:16.7 and roasting at 187 °C for 60 min effectively reduced NH_4^+ and Mn to below discharge standards while also addressing the leachate's magnesium hazard (MH). Mechanistic analyses revealed that the roasting process facilitated the conversion of dihydrate gypsum to hemihydrate gypsum, with Mn^{2+} and Mg^{2+} primarily immobilized as MnO and $Mg(OH)_2$, respectively. This approach offers a cost-effective and efficient solution for EMR treatment, contributing to sustainable electrolytic manganese metal production practices [96–98].

4. Thermodynamic Analysis of EMR

The thermodynamic analysis involves studying the energy changes and transformations that occur during a chemical process [5,99]. In the case of EMR, we can analyze its utilization's thermodynamics to understand the process's feasibility and energy requirements [100]. Additionally, in the thermodynamic analysis of the utilization of EMR, the specific reactions and calculations may vary depending on the composition of the residue and the desired utilization products [100–102]. The Van't Hoff equation [103] enables the computation of thermodynamic parameters such as the Gibbs Free Energy (ΔG), enthalpy (ΔH), and entropy (ΔS) using the mathematical expressions in Equations (49) and (50) [104].

$$\ln K_L = -\frac{\Delta H}{RT} + \frac{\Delta S}{R} \quad (49)$$

$$\Delta G = \Delta H - T\Delta S \quad (50)$$

where ΔH represents the alteration in enthalpy (KJ mol^{-1}), ΔS represents the shift in entropy (J mol^{-1} K^{-1}), ΔG represents the change in Gibbs free energy (KJ mol^{-1}), K_L represents the adsorption equilibrium constant (L mol^{-1}), R is the gas constant (8.314 J mol^{-1} K^{-1}), and T represents the gas constant (K).

Researchers have conducted extensive thermodynamic analyses to elucidate the behavior of EMR under various conditions, intending to optimize its utilization pathways. A study by He et al. [19] examines how ammonium sulfate and pyrite phases break down and change within the EMR through a roasting process. The optimal conditions for this process were identified as 120 min at 550 °C, 60 min at 600 °C, and 30 min at 650 °C. Their research employed HSC Chemistry 9.0 (HSC Chemistry, 2019) to determine the reaction equilibrium in phase transformation during the roasting process. This was achieved by minimizing Gibbs free energy under conditions that were isobaric, isothermal, and involved unit moles target reactants like FeS_2(s), $MnCO_3$(s), $CaSO_4 \cdot 2H_2O$(s), $MgCO_3$(s), and $(NH_4)2SO_4$(s).

Duan et al. [105] employed thermodynamic modeling techniques to study the kinetics of phase transformations in EMR during calcination. Their research highlighted the importance of temperature and reaction conditions in controlling the thermodynamic behavior of EMR-derived products, thereby guiding process optimization efforts. Wu et al. [106] investigated the thermodynamic stability of mesoporous spinel manganese oxide synthesized from EMR. Their findings reveal the importance of thermodynamic considerations in designing materials with enhanced catalytic performance and stability.

4.1. Kinetic Model and Phase Transformation Characteristics EMR

The leaching of manganese in EMR under a sulphuric acid system is typically categorized as a solid-liquid heterogeneous reaction. The primary chemical reactions involved are as follows:

$$2MnO_2 + 2H_2SO_4 \leftrightarrow 2MnSO_4 + O_2 \uparrow + 2H_2O \quad (51)$$

$$MnO + H_2SO_4 \leftrightarrow MnSO_4 + H_2O \quad (52)$$

$$MnCO_3 + H_2SO_4 \leftrightarrow MnSO_4 + H_2O + CO_2 \quad (53)$$

The intricate chemical mechanism involves sulfuric acid and an EMR matrix where manganese is leached. Importantly, it draws attention to the fact that the response mechanisms at various locations exhibit differing degrees of symmetry, as depicted in Figure 5.

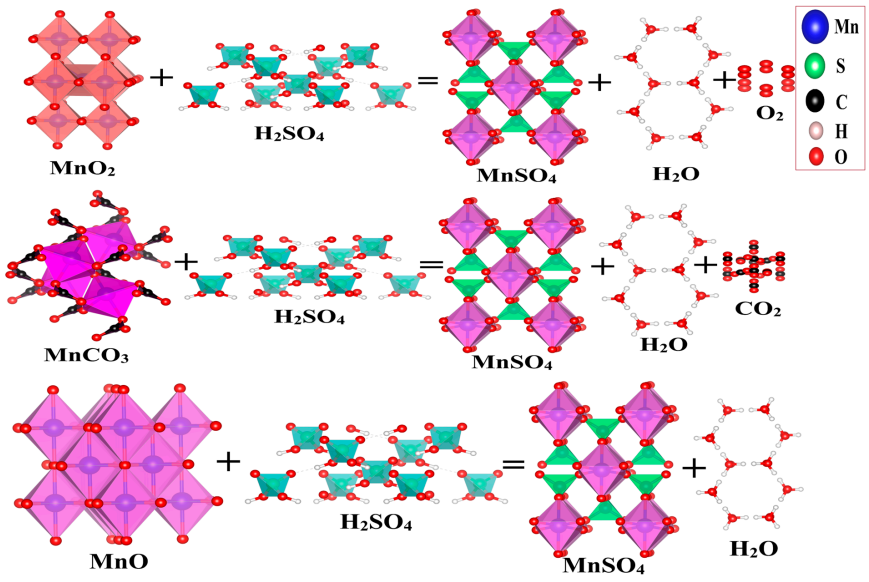

Figure 5. Structure symmetry ofsolid-liquid heterogeneous mechanism reactions under sulfuric acid leaching kinematics.

Zhang et al. [107] conducted a study to explore the feasibility of using EMAS via SO_2 roasting and acid leaching, analyzing it through thermodynamic calculations. Their thermodynamic analysis revealed that $MnSO_4$ and $PbSO_4$ coexist during the roasting and leaching processes, allowing their separation based on differing solubilities. The primary stages of the roasted products consisted of Mn_3O_4, $MnSO_4$, and $PbSO_4$. The optimal conditions resulted in a leaching efficiency of 92.5% for Mn and just 3.21% for Pb, demonstrating an efficient method for utilizing EMAS by effectively separating manganese and lead.

4.2. Oxidation of Manganese Oxide in EMR

Various experimental techniques and theoretical models have been employed to elucidate the oxidation mechanisms and kinetics of manganese oxide in EMR [47,108,109]. The main reactions are depicted in Equations (54) and (55), while the related changes in manganese oxide and energy are presented in Table 3. The phase transformation for the thermodynamic analyses is depicted in Table 4.

$$\text{Reaction 1; } MnO(s) + 1/2O_{2(g)} \rightarrow MnO_2(s) \quad (54)$$

$$\text{Reaction 2; } 2MnO(s) + O_{2(g)} \rightarrow 2MnO_2(s) \quad (55)$$

Table 3. Reactions of different reducing agents, MnO_2, and corresponding ΔG_T^θ equations.

Reaction Equation	ΔG_T^θ (kJ·mol^{-1})	Spontaneous Reaction/ Temperature Range/K
$11MnO_2 + 2FeS_2 = 11MnO + Fe_2O_3 + 4SO_{2(g)}$	$\Delta G_T^\theta = -170.92 - 1.026T$	Spontaneous
$15MnO_2 + 2FeS_2 + 14H_2SO_4 = 15MnSO_4 + Fe_2(SO_4)_3 + 14H_2O$	$\Delta G_T^\theta = -2918.36 - 0.014T$	Spontaneous
$2MnO_2 + SO_{2(g)} = Mn_2O_3 + SO_3(l)$	$\Delta G_T^\theta = -15.01 + 0.018T$	T < 834
$3MnO_2 + 2SO_{2(g)} = Mn_3O_4 + 2SO_3(l)$	$\Delta G_T^\theta = -22.22 + 0.049T$	T < 453
$MnO_2 + SO_{2(g)} = MnSO_4$	$\Delta G_T^\theta = -240.98 + 0.177T$	T < 1361
$3MnO_2 + 2Fe + 6H_2SO_4 = 3MnSO_4 + Fe_2(SO_4)_3 + 6H_2O$	$\Delta G_T^\theta = 1020.13 + 0.047T$	Spontaneous

Table 4. Phase transformation and reaction during SO_2 roasting and corresponding ΔG_T^θ equations [107].

Reaction Equation	ΔG_T^θ (kJ·mol^{-1})	Spontaneous Reaction/Temperature Range/K
$MnO_2 + SO_{2(g)} = MnSO_4$	$\Delta G_T^\theta = -192.7 + 0.18T$	T < 1091
$2MnO_2 = Mn_2O_3 + 1/2O_{2(g)}$	$\Delta G_T^\theta = 55.64 - 0.1T$	T > 530.5
$3MnO_2 + SO_{2(g)} = Mn_2O_3 + MnSO_4 + 1/2O_{2(g)}$	$\Delta G_T^\theta = -32.76 + 0.02T$	T < 1910
$2Mn_2O_3 + SO_{2(g)} = Mn_3O_4 + MnSO_4$	$\Delta G_T^\theta = -43.35 + 0.05T$	T < 963.3
$Mn_2O_3 + 2SO_{2(g)} + 1/2O_{2(g)} = 2MnSO_4$	$\Delta G_T^\theta = -441.4 + 0.46T$	T < 962.7
$Mn_3O_4 + 3SO_{2(g)} + O_{2(g)} = 3MnSO_4$	$\Delta G_T^\theta = -700.8 + 0.73T$	T < 964.3
$2Mn_3O_4 + 6SO_{2(g)} = 5MnSO_4 + MnS$	$\Delta G_T^\theta = -156.7 + 0.26T$	T < 602.7
$4Mn_2O_3 + 8SO_{2(g)} = MnS + 7MnSO_4$	$\Delta G_T^\theta = -243.4 + 0.35T$	T < 695.4
$Mn_3O_4 + SO_{2(g)} = 2MnO + MnSO_4$	$\Delta G_T^\theta = -24.41 + 0.04T$	T < 642.4
$PbO2 + SO_{2(g)} = PbSO_4$	$\Delta G_T^\theta = -291.2 + 0.17T$	T < 1730
$PbO2 = PbO + 1/2O_{2(g)}$	$\Delta G_T^\theta = 9.10 - 0.02T$	T < 441.4
$PbO + SO_{2(g)} + 1/2O_{2(g)} = PbSO_4$	$\Delta G_T^\theta = 78.70 + 0.06T$	T < 1256
$4PbO + 4SO_{2(g)} = PbS + 3PbSO_4$	$\Delta G_T^\theta = -142.0 + 0.17T$	T < 843.3

In summary, the chemical equation of the EMR utilization process and thermodynamic calculations offer valuable insights into the mechanisms and energy transformations involved in effectively harnessing EMR. By studying the chemical reactions and energy transfers associated with EMR, we gain a deeper understanding of this process's fundamental principles. Utilizing EMR presents a significant opportunity for sustainable resource

management and recovering valuable materials. By exploring the chemical equation of the EMR utilization process, we can identify the essential reactions and transformations during the recovery and utilization of manganese and other valuable components. Thermodynamic calculations play a crucial role in assessing the feasibility and efficiency of the EMR utilization process. We can evaluate the process's energy requirements, losses, and overall efficiency by applying thermodynamic principles. These calculations enable us to optimize the operating conditions, determine the appropriate temperatures, pressures, and reactant concentrations, and maximize the extraction and utilization of valuable resources from EMR.

5. Resource Utilization of EMR

The reduction and pre-treatment of EMR can mitigate pollution by minimizing land occupation and lowering the risk of secondary pollution. However, to address EMR pollution more effectively, reutilization strategies must be implemented. These strategies include recycling valuable resources contained within EMR and employing them in various applications such as construction engineering and other applications, summarized in Tables 5 and 6. The surging demand in the construction sector for vital resources like concrete, cement, bricks, and subgrade materials offers a ripe opportunity for adopting EMR reuse. EMR strategies involve repurposing and recycling these materials, serving as a sustainable solution to curb waste and environmental impact. By embracing EMR practices, the construction industry can address concerns regarding resource scarcity while fostering innovation and efficiency. EMR contains quartz, aluminosilicate, and gypsum, which align with the raw material requirements for construction. Leveraging EMR in this way enhances its comprehensive utilization and contributes to resource conservation.

5.1. EMR in Building Materials

5.1.1. EMR in Cementitious Materials

Recent studies have shown that EMR can be versatile in cementitious materials, serving as a retarder, light aggregate, activator, and mineralizer. Its incorporation into cement production can lead to cost savings and significant consumption of EMR, addressing both economic and environmental concerns. The primary minerals in Portland cement, such as C_2S ($2CaO{\cdot}SiO_2$, dicalcium silicate), C_3S ($3CaO{\cdot}SiO_2$, tricalcium silicate), C_3A ($3CaO{\cdot}Al_2O_3$, tricalcium aluminate), and C_4AF ($3CaO{\cdot}Al_2O_3{\cdot}Fe_2O_3$, tetracalcium aluminoferrite), can be synthesized by calcining a mixture of EMR, clay, and limestone. Various cement types, including Portland, quasi-sulfoaluminate, and specialized EMR cement, have been successfully produced with EMR content ranging from 2% to 40% [110–113]. However, the use of EMR in cement is limited by its high ammonia (NH_4^+) and sulfate (SO_4^{2-}) content. Incomplete treatment can lead to environmental issues due to ammonia release and may affect cement stability if sulfur oxide levels exceed industry standards. Therefore, while EMR presents a valuable resource for the cement industry, its incorporation must be carefully managed to mitigate environmental risks and ensure product quality, maintaining EMR content within the optimal range of 3% to 5% to prevent adverse effects. Table 5 outlines the use of EMR in the preparation of cement or cementing materials [114]. Figure 6 illustrates various preparation processes for cement or cement-based products incorporating EMR.

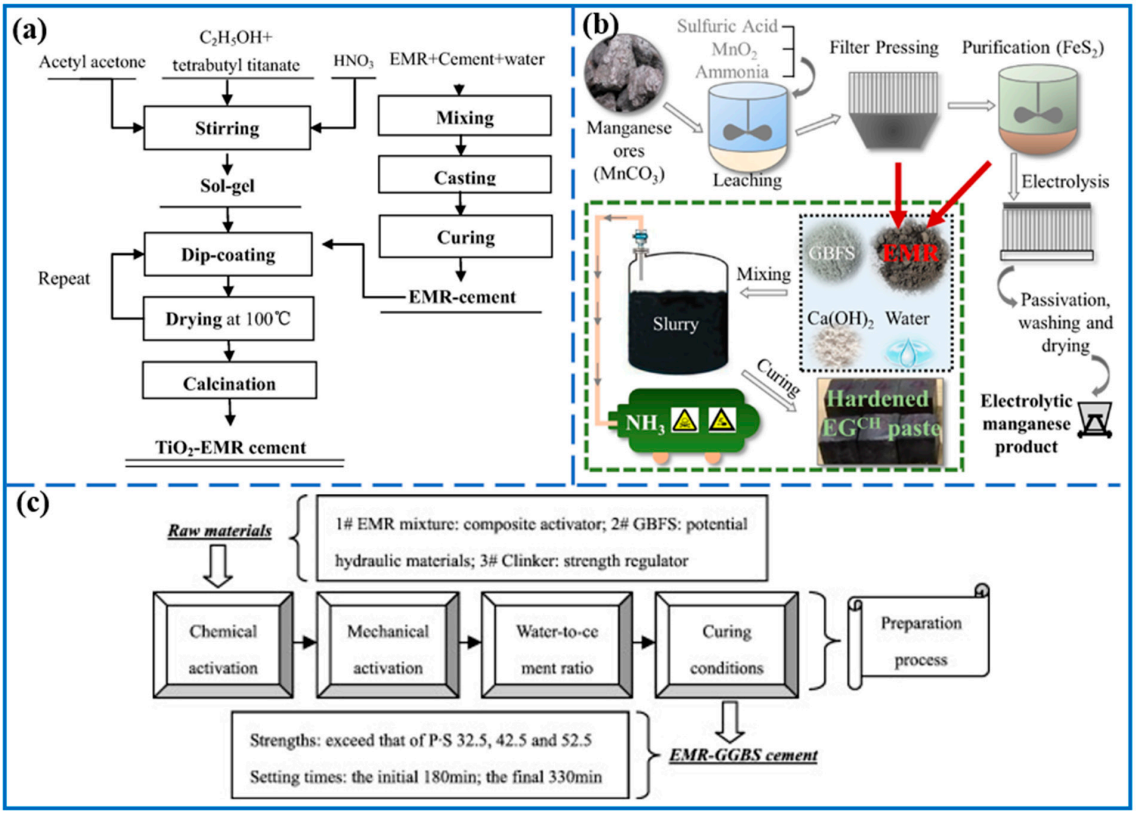

Figure 6. Schematic for the preparation of cement or cement-related products containing EMR: (**a**) TiO_2-EMR cement referred from [115] (**b**) EG^{CH} hardened EMR cementitious material, referred from [14] (**c**) EMR-GBFS cement, referred from [113].

5.1.2. Bricks and Road Base Materials

The utilization of solid waste materials as substitutes for traditional construction materials like clay has garnered significant attention in recent years. Various types of bricks and road bases have been developed using EMR, offering promising properties such as good splitting tensile strength, compressive strength, and permeability coefficient. Examples include autoclaved bricks, baking-free bricks, non-sintered permeable bricks, and non-burnt permeable bricks, which can incorporate a significant percentage of waste materials.

Although these technologies demonstrate promise, their industrialization faces hurdles such as the substantial costs of NH_3 receiving facilities and the lack of demand in local building materials markets. EMR exhibits significant pozzolanic properties, making it suitable for utilization as a primary material in brick manufacturing. Researchers have explored various formulations and processes to manufacture bricks with desirable properties. For instance, researchers have successfully produced sintered bricks with impressive compressive strength (ranging from 24.34 to 30.72 MPa) by incorporating blends of EMR, fly ash, and shale [116]. Non-burning bricks have also been prepared by solidifying EMR with lime, water, and ordinary Portland cement, resulting in products meeting industry standards and exhibiting reduced heavy metal leaching [111,116] (See Table 5).

Additionally, permeable bricks, known for their environmental friendliness and ease of production, have been developed using EMR and additives mixed into mud. By incorporating blast furnace slag, cement, stone, and water, these bricks can be formed without high-temperature sintering [117,118]. They demonstrate satisfactory mechanical properties and environmental compatibility. Industrial CT has been employed to analyze these bricks' internal void structure and water permeability, revealing promising results [119]. Table 6 outlines the use of EMR in the preparation of bricks and road-based materials.

In summary, using waste materials like EMR in construction offers opportunities to produce environmentally friendly and cost-effective building materials, although further

research and overcoming logistical challenges are necessary for widespread adoption in industrial applications. Further exploration into the application of EMR for road construction holds considerable promise. This approach presents an opportunity to effectively utilize EMR in substantial quantities and integrate it with other industrial solid wastes like red mud and calcium carbide slag to fabricate road-based materials. These resulting materials demonstrate favorable characteristics such as enhanced unconfined compressive strength and efficient solidification of heavy metal elements. Given the potential for widespread implementation, the future integration of EMR into road-based materials holds significant potential.

Table 5. Brief summary of cementitious materials prepared by EMR.

References	Product Compositions (wt.%)	Product Characteristics	Leaching Toxicity (mg/L)
[120]	EMR: 12%, hot-stewed steel slag: 28%, cement: 60%	Cementitious materials: Compressive strength: 50.5 MPa, flexural strength: 8.0 MPa	-
[121]	EMR: 13.5%, NaOH: 1.5%	Cement admixture: Compressive strength: 10.03 MPa	Cd: 0.0035, Ni: 0.1565, Zn: 0.1886, Cr: 0.0877, Mn: 0.5321, Pb: 0.1346
[122]	EMR: 20~35%, sulfur: 45~55%, sand: 15~30%	Sulfur concrete: Compressive strength: 48.89~63.17 MPa, flexural strength: 7.12~9.47 MPa	Cd: N.D., Cu: 0.004, Zn: 0.043, Cr: 0.033, Ni: 0.030, Mn: 0.045, Pb: 0.034
[120]	EMR: 14%, hot-stewed steel slag: 36%, cement: 50%,	Cementitious materials: Compressive strength: 43.5 MPa, flexural strength: 7.0 MPa	-
[115]	Preparation: EMR: 8% TiO_2 coating: absolute ethanol, water, and HNO_3 coat on the cement	TiO_2-EMR cement materials: compressive and flexural strength meet the national standard	Mn: 0.515, Cu: N.D., Cd: N.D., Zn: 0.086 Pb: 0.094, Cr: N.D
[123]	EMR (be pretreated with carbide slag): 15%, clinker: 65%, blast furnace slag: 20%	Cement-based cementitious material: Compressive strength: 32.9 MPa, flexural strength: 6.8 MPa	Mn < 0.001, Cd < 0.001, As < 0.001, Cr: 0.053, NH_4^+N: 1.56, Pb: 0.003
[14]	EMR: 45%, GBFS: 50%, $Ca(OH)_2$: 5%	Cementitious material: Compressive strength: 30 MPa	Mn: N.D., NH_4^+N < 0.175 mmol/L
[124]	EMR: 10–40%, limestone: 60–70%, kaolin: 0–20%, gypsum: 5%	Quasi-sulphoaluminate cementitious material: Compressive strength: 35–65 MPa	-
[125]	EMR: 5%, fly ash: 10%, blast furnace slag 10%,	The compressive strength and flexural strength exhibit an initial increase (0–5%) followed by a drop (5–20%) when the EMR increases. EIF90 of 5.4 $kg{\cdot}MPa^{-1}{\cdot}m^3$	-
[113]	Activator (EMR:$Ca(OH)_2$:clinker = 30:3:5): 20~35%, GBFS: 30~65%, clinker > 5%	Preparation of electrolytic manganese residue–ground granulated blast furnace slag cement	-

N.D.; Not Detected.

Table 6. Brief summary of bricks prepared by EMR.

References	Product Compositions (wt.%)	Product Characteristics	Leaching Toxicity (mg/L)
[126]	EMR: 42.7%, red mud: 21%, aggregate: 15%, cement: 5%, carbide slag 6.3%	Non-sintered bricks: Absorption band: 1621–1675 cm^{-1}	NH_{4+}-N: N.D.
[75]	EMR: 30%, aggregate: 59.5%, cement: 10.5%	Steam-autoclaved bricks: Compressive strength: 22.05 MPa, binding strength: 5.76 MPa	Mn: N.D., Hg^{2+}: 4.4×10^{-4}, Pb^{2+}: 0.127, Cd^{2+}: 0.010, Ba^{2+} N.D., Ni^{2+} N.D., Ag^+ N.D., Cd^{2+} 0.010 Cr^{3+} N.D., Cr^{6+} N.D., Cu^{2+}: 0.015, Zn^{2+}: 0.029, Be^{2+}: 0.015

Table 6. *Cont.*

References	Product Compositions (wt.%)	Product Characteristics	Leaching Toxicity (mg/L)
[111]	Pretreated EMR: 30–40%, aggregate: 40–60%, cement: 10.5–12%	Steam-autoclaved bricks: Compressive strength: >15 MPa, dry shrinkage: <0.11%	Mn: N.D., Cd: 0.01, As: 1.23×10^{-3}, Cr: N.D., Cu: 0.015, Hg: 4.4×10^{-4}, Pb: 0.127
[127]	EMR: 63%, sand: 10%, $Ca(OH)_2$: 12% thermal-mechanical activated K-feldspar: 15%	Autoclaved brick: Compressive strength: 23.5 MP	Mn: <0.02
[118]	EMR: 30%, additive: 8%	Permeable bricks: Splitting tensile strength: 3.53 MPa, permeability coefficient: 3.2×10^{-2} cm/s	Mn: N.D., Cd: N.D., As: N.D., Cr: N.D., Hg: N.D., Pb: N.D., NH_{4+}-N: N.D.
[116]	EMR: 90%, shale: 5–10%, coal ash: 0–5%	Sintered bricks: Compressive strength: 24.34–30.72 MPa,	-
[119]	Surface material: Cement: 15%, pigment: 3%, stone: 75%, water: 7% Base material: EMR: 15%, stone: 72%, cement: 3%, additives: 7%, water: 3%	Permeable bricks: Splitting tensile strength: 3.85 MPa, permeability coefficient: 3.2×10^{-2} cm/s	-
[128]	EMR: 100%	Baking-free bricks: Compressive strength > 12 MPa	Mn: N.D., NH_4^+-N: N.D
	EMR: 50%, river sand: 25%, quicklime: 10%, cement: 15%	Baking-free brick: Compressive strength: 19 MPa	-
[129]	EMR: 60%, standard sand: 20%, cement: 20%	Autoclaved brick: Resistance to break intensity: 4.4 MPa, resistance to pression intensity: 23.8 MPa	Zn: 0.33, Cu: 0.30, Hg: 0.018, Pb:1.9, Cr^{3+}: 0.05, Cr^{6+}: N.D., Cd: 0.02, As: 0.12, F: 0.11, Ni: 0.58
[130]	Pretreated EMR: 30% (EMR: lime = 8:1 (g/g)), water: 30%, cement: 10.5%, aggregate: 59.5%	Autoclaved brick: Compressive strength: 22.05 MPa, binding strength: 5.75 MPa	Mn: N.D., Cd: 0.01, As: 1.23×10^{-3}, Cu: 0.015, Hg: 4.4×10^{-4}, Pb: 0.127, Zn: 0.029, F: 0.052, Be: 0.015, Se: 5.56×10^{-3}
[117]	EMR: 60%, river sand: 20%, cement:20%	Unfired EMR brick: Compressive strength: 42.6 MPa, water absorption rate: 6.5%, bulk density 1.9370~2.0239 g/cm^3	Mn: 1.2, Pb: <0.01, Zn: 0.12 Co: 0.01, As: 0.41 Fe: 086

N.D.; Not Detected.

5.1.3. Ceramics Materials

In addressing industrial solid waste management, the transformation of Electrolytic EMR into aluminosilicate-based glass-ceramics and ceramics has gained significant traction [131,132]. The calcination of EMR without modification can produce CaO-MgO-Al_2O_3-SiO_2 series glass-ceramics with a crystallization activation energy of merely 429.00 kJ/mol, as highlighted by [133]. These materials, including anorthite and enstatite multiphase ceramics, demonstrate superior mechanical qualities such as bulk density, bending strength, and compressive strength, achieved with EMR incorporation ranging from 10% to 35% [52,133]. Furthermore, the development of ceramisite from EMR, meeting the environmental safety standards (GB/T 1743.1-2010), marks a significant stride in EMR reuse, supporting the creation of non-hazardous, lightweight aggregates [134–136].

In parallel developments, Wu et al. [137] demonstrated using talc, bauxite, and quartz alongside EMR to manufacture ceramics at temperatures ranging from 1100 to 1200 °C. These products exhibited notable mechanical properties and were suitable for thermal insulation and high-temperature applications. Similarly, studies by Zhang et al. [138] and Hu & Yu [139] have shown the feasibility of integrating 30–40% EMR into the production of ceramic tiles, effectively isolating heavy metal contaminants within the ceramic structure. Cheng et al. [140] synthesized a porous material based on EMR, achieving a compressive

strength of 6.55 MPa. This synthesis occurred at 1170 °C for 50 min, with silicon carbide (SiC) employed as a pore-forming agent. Increased SiC addition resulted in a decline in the compressive strength of the porous material. Zhan et al. [141] devised a method to produce lightweight ceramsite by blending EMR, fly ash, and MSW fly ash. They purified the MSW fly ash through a heating process at a controlled rate of 10 °C per minute, reaching a temperature of 1160 °C for 12 min. The resulting ceramics met the requirements for Class 800 lightweight aggregates and demonstrated effective encapsulation of heavy metals.

These scholarly contributions illuminate the versatility and environmental compatibility of EMR-based materials, offering substantial opportunities for waste reduction and resource recovery in the industrial sector. The integration of EMR mitigates the environmental footprint associated with manganese production and introduces innovative applications in the construction and manufacturing industries, underscoring the need for ongoing research into these materials' optimization and environmental impacts.

5.1.4. Agriculture (Organic Fertiliser)

Amidst the growing global demand for soil fertilizers to sustain agricultural productivity [142], the utilization of waste materials like EMR offers a sustainable solution. Urban industrial waste, often rich in nutrients vital for crop growth, can be effectively repurposed for fertilizer production, mitigating environmental damage and reducing production costs [143,144]. In modern agriculture, EMR stands out as a valuable resource for fertilizer production. EMR is Rich in Mn and plays a crucial role in supporting crop vitality, directly engaging in essential processes such as photosynthesis and enzyme activation [39]. Notably, its high manganese content, primarily in sulfate form, renders it ideal for agricultural fertilizer production [145].

Researchers have explored various methods to harness the potential of EMR in fertilizer production. Wang et al. [146] demonstrated the synthesis of compound fertilizer granules by mixing EMR with steel slag and water, achieving favorable agricultural outcomes. Additionally, Jiang et al. [147] revealed a process involving the EMR alkaline treatment to convert silica (SiO_2) into silicate, thereby producing silica-manganese fertilizer. These endeavors resulted in elevated silicon content, enhancing the efficacy of the fertilizer [91]. A parallel study by Lv et al. [82] activated Si in EMR utilizing silicate microorganisms. The experimental findings indicated that the bioleaching solution contained 163.27 mg/L of silicon, which possesses the potential to serve as a viable silicon fertilizer resource.

Furthermore, the utility of EMR extends beyond its manganese content. Fertilizers produced from EMR offer vital nutrients, including nitrogen, potassium, phosphorus, and ammonium nitrogen, which are indispensable for promoting vigorous crop growth [148,149]. Additionally, EMR aids in fortifying crops against environmental stressors like lodging, insects, drought, and diseases, ultimately boosting crop yields [148]. In summary, Incorporating EMR into organic fertilizer formulations represents a strategic approach toward sustainable agriculture. Nevertheless, heavy metal ions within EMR-based organic fertilizers introduce environmental and human health concerns. Heavy metals, including manganese, can exert toxic effects on plant roots, impairing their growth and overall health. Additionally, these metals possess the potential to leach into the surrounding soil and water, thereby causing contamination and posing significant risks to ecosystems and human populations alike. Therefore, enhancing the safe handling of heavy metals in EMR is essential, leading to increased usage of EMR consumption in agriculture.

5.1.5. EMR in Other Applications

The composition of EMR presents an opportunity for diverse applications. With SiO_2 content ranging from 22.03–41.24% and Al_2O_3 ranging from 2.27–8.54%, EMR serves as a valuable resource for the synthesis of adsorbents like zeolite [36,150–153], mesoporous silica and other absorbents [70,154], in geopolymer [155–158]. Additionally, there has been a growing preference for the utilization of adsorbents in wastewater treatment due to their simplicity, efficiency, long-term viability, and renewable nature [159]. However,

industrial, urban, and agricultural wastes possess chemical and structural compositions that are suitable for wastewater treatment. Utilizing these wastes, offers the potential to prepare effective treatment materials [160]. If implemented, this approach can potentially lower the manufacturing expenses associated with wastewater treatment materials, as Hossain et al. [161] emphasized. Moreover, it guarantees the utilization of these wastes, thereby contributing to a reduction in environmental degradation. EMR has been investigated in recent studies for its potential use in wastewater disposal or as a catalyst support technology [162,163].

These investigations have offered insights into the potential reuse of substantial quantities of EMR. However, the limited focus has been on exploring the leaching toxic effects, longevity, micro-properties, and the solidification technique of heavy metallic ions in the EMR. The utilization of EMR in wastewater treatment is considered a minor application for several reasons. These include the limited quantity of EMR utilized, the complexity of the production process involved, and the inadequate exploration of the solidification mechanism for other heavy-metal ions. Despite its potential benefits, these factors hinder the use of EMR in wastewater treatment, highlighting the need for further research and development to overcome existing challenges and fully leverage its effectiveness in this area.

6. Conclusions and Areas of Future Study

This review systematically explores the multifaceted aspects of EMR, including its environmental challenges, recovery methodologies, and utilization strategies. The research revealed the significance of EMR as both a liability and a resource, highlighting advancements in treatment processes such as water-leaching, chemical-leaching, alkaline-leaching, bioleaching, and roasting. The integration of thermodynamic and kinetic models has illuminated the mechanisms behind EMR treatment, facilitating the development of more effective recovery methods. Furthermore, the potential application of EMR in construction materials opens new avenues for sustainable waste management.

6.1. Prospects and Technical Aspects

The focus on EMR treatment and utilization should pivot towards innovation in process efficiency, environmental sustainability, and economic viability. Integrating advanced technologies, such as nanotechnology and biotechnology, could open new pathways for the enhanced recovery of valuable metals and the development of high-value products from EMR. Exploring novel bioleaching microbes and genetically engineered strains could improve leaching efficiencies and selectivity for specific metals. Innovations could include optimizing existing methodologies and exploring novel treatment technologies such as membrane or advanced oxidation processes, offering a promising avenue for selective metal recovery.

6.2. Policy and Market

Strengthened regulatory frameworks are essential for the promotion of EMR recycling and utilization. Policies should encourage the development of environmentally friendly and cost-effective EMR treatment technologies. Furthermore, regulations should facilitate the safe use of EMR-derived products in various industries, ensuring they meet stringent environmental and health standards.

The market for EMR-derived products, particularly in the construction and materials sectors, needs further development. Market analyses should identify potential applications and demand for EMR-based products, guiding research and development efforts. Public awareness campaigns can also play a critical role in increasing market acceptance and demand for recycled materials.

6.3. Environmental Sustainability and Economic Evaluation

Efforts should be directed toward minimizing the environmental footprint of EMR treatment processes and maximizing the beneficial use of recovered materials. Lifecycle assessments can provide insights into the environmental impacts of different treatment options, guiding the selection of sustainable methodologies. Promoting the circular economy through integrating EMR into new products can significantly reduce waste and resource consumption. Economic evaluations are crucial for assessing the viability of EMR treatment processes and their derived products. Cost-benefit analyses should consider the entire lifecycle of EMR, from treatment to end-use applications. Economic incentives, such as subsidies or tax breaks, could be implemented to encourage investment in EMR treatment facilities and the development of EMR-based products. Adapting to the global solid waste issue of EMR and the sustainable development of the EMM sector is of considerable scientific importance, and this review paper is anticipated to offer theoretical solid support for the clean disposal and efficient exploitation of EMR.

Author Contributions: A.L.: Investigation, Methodology, Writing—original draft, Writing—review & editing, Conceptualization, Validation. X.C.: Supervision, Funding acquisition, Resources, Project administration, Software, Validation. S.M.K.: Data curation, Visualization, Writing—review & editing. T.F.: Data curation, Conceptualization, Writing—review & editing. All authors have read and agreed to the published version of the manuscript.

Funding: The authors are grateful for the support from the Scientific Research Development Foundation Fund of Zhengzhou University (grant number 25124510001) and the Key Research Project of Henan Province (grant number 212102311161).

Conflicts of Interest: The authors declare no conflicts of interest.

References

1. Clarke, C.; Upson, S. A global portrait of the manganese industry—A socioeconomic perspective. *Neurotoxicology* **2017**, *58*, 173–179. [CrossRef] [PubMed]
2. Liu, B.; Zhang, Y.; Lu, M.; Su, Z.; Li, G.; Jiang, T. Extraction and separation of manganese and iron from ferruginous manganese ores: A review. *Miner. Eng.* **2019**, *131*, 286–303. [CrossRef]
3. Elliott, R.; Coley, K.; Mostaghel, S.; Barati, M. Review of Manganese Processing for Production of TRIP/TWIP Steels, Part 1: Current Practice and Processing Fundamentals. *JOM* **2018**, *70*, 680–690. [CrossRef]
4. Steenkamp, J.D.; Bam, W.G.; Ringdalen, E.; Mushwana, M.; Hockaday, S.A.C.; Sithole, A.N. Working towards an increase in manganese ferroalloy production in South Africa—A research agenda. *J. S. Afr. Inst. Min. Metall.* **2018**, *118*, 645–654. [CrossRef]
5. Sun, D.; Yang, L.; Liu, N.; Jiang, W.; Jiang, X.; Li, J.; Yang, Z.; Song, Z. Sulfur resource recovery based on electrolytic manganese residue calcination and manganese oxide ore desulfurization for the clean production of electrolytic manganese. *Chin. J. Chem. Eng.* **2020**, *28*, 864–870. [CrossRef]
6. Zhang, R.; Ma, X.; Shen, X.; Zhai, Y.; Hong, J. Life cycle assessment of electrolytic manganese metal production. *J. Clean. Prod.* **2020**, *253*, 119951. [CrossRef]
7. Lan, J.; Sun, Y.; Tian, H.; Zhan, W.; Du, Y.; Zhang, T.; Hou, H. Electrolytic manganese residue-based cement for manganese ore pit backfilling: Performance and mechanism. *J. Hazard. Mater.* **2021**, *411*, 124941. [CrossRef]
8. Zhang, Y.; Liu, X.; Xu, Y.; Tang, B.; Wang, Y. Preparation of road base material by utilizing electrolytic manganese residue based on Si-Al structure: Mechanical properties and Mn^{2+} stabilization/solidification characterization. *J. Hazard. Mater.* **2020**, *390*, 122188. [CrossRef]
9. Han, F.; Wu, L. *Industrial Solid Waste Recycling in Western China*; Springer Nature Singapore Pte Ltd.: Singapore, 2019. [CrossRef]
10. Tian, Y.; Shu, J.; Chen, M.; Wang, J.; Wang, Y.; Luo, Z.; Wang, R.; Yang, F.; Xiu, F.; Sun, Z. Manganese and ammonia nitrogen recovery from electrolytic manganese residue by electric field enhanced leaching. *J. Clean. Prod.* **2019**, *236*, 117708. [CrossRef]
11. He, D.; Luo, Z.; Zeng, X.; Chen, Q.; Zhao, Z.; Cao, W.; Shu, J.; Chen, M. Electrolytic manganese residue disposal based on basic burning raw material: Heavy metals solidification/stabilization and long-term stability. *Sci. Total Environ.* **2022**, *825*, 153774. [CrossRef]
12. Wang, F.; Long, G.; Bai, M.; Wang, J.; Zhou, J.L.; Zhou, X. Application of electrolytic manganese residues in cement products through pozzolanic activity motivation and calcination. *J. Clean. Prod.* **2022**, *338*, 130629. [CrossRef]
13. Wu, F.; Liu, X.; Qu, G.; Ning, P. A critical review on extraction of valuable metals from solid waste. *Sep. Purif. Technol.* **2022**, *301*, 122043. [CrossRef]
14. Wang, D.; Wang, Q.; Xue, J. Reuse of hazardous electrolytic manganese residue: Detailed leaching characterization and novel application as a cementitious material. *Resour. Conserv. Recycl.* **2020**, *154*, 104645. [CrossRef]

15. Han, F.; Wu, L. Resource Utilization of Electrolytic Manganese Residues. In *Industrial Solid Waste Recycling in Western China*; Springer: Singapore, 2019; pp. 127–164. Available online: http://link.springer.com/10.1007/978-981-13-8086-0_3 (accessed on 10 May 2024).
16. Xu, F.; Jiang, L.; Dan, Z.; Gao, X.; Duan, N.; Han, G.; Zhu, H. Water balance analysis and wastewater recycling investigation in electrolytic manganese industry of China—A case study. *Hydrometallurgy* **2014**, *149*, 12–22. [CrossRef]
17. Xu, L.; Wang, X.; Chen, H.; Liu, C. Mn forms and environmental impact of electrolytic manganese residue. *Adv. Mat. Res.* **2011**, *183–185*, 570–574. [CrossRef]
18. Zhang, X.; Wang, P.; Li, J.; Gao, Y.; Liu, S.; Wang, C.; Onyekwena, C.C.; Lei, X. Exploring the migration and transformation behaviors of heavy metals and ammonia nitrogen from electrolytic manganese residue to agricultural soils through column leaching test. *Environ. Sci. Pollut. Res.* **2023**, *30*, 93199–93212. [CrossRef] [PubMed]
19. He, S.; Jiang, D.; Hong, M.; Liu, Z. Hazard-free treatment and resource utilisation of electrolytic manganese residue: A review. *J. Clean. Prod.* **2021**, *306*, 127224. [CrossRef]
20. Yamaguchi, T.; Nagano, H.; Murai, R.; Sugimori, H.; Sekiguchi, C.; Sumi, I. Development of Mn recovery process from waste dry cell batteries. *J. Mater. Cycles Waste Manag.* **2018**, *20*, 1909–1917. [CrossRef]
21. Jacob, R.; Sankaranarayanan, S.R.; Babu, S.K. Recent advancements in manganese steels—A review. *Mater. Today Proc.* **2020**, *27*, 2852–2858. [CrossRef]
22. Sun, X.; Hao, H.; Liu, Z.; Zhao, F. Insights into the global flow pattern of manganese. *Resour. Policy* **2020**, *65*, 101578. [CrossRef]
23. Shu, J.; Liu, R.; Liu, Z.; Chen, H.; Tao, C. Enhanced extraction of manganese from electrolytic manganese residue by electrochemical. *J. Electroanal. Chem.* **2016**, *780*, 32–37. [CrossRef]
24. Wang, F.; Long, G.; Ma, K.; Zeng, X.; Tang, Z.; Dong, R.; He, J.; Shangguan, M.; Hu, Q.; Liew, R.K. Recyling manganese-rich electrolytic residues: A review. *Environ. Chem. Lett.* **2023**, *21*, 2251–2284. [CrossRef]
25. Yang, T.; Xue, Y.; Liu, X.; Zhang, Z. Solidification/stabilization and separation/extraction treatments of environmental hazardous components in electrolytic manganese residue: A review. *Process Saf. Environ. Prot.* **2022**, *157*, 509–526. [CrossRef]
26. Wang, Q.; Wang, S.; Ma, X.; Cao, Z.; Zhang, C.; Zhong, H. A green production process of electrolytic manganese metal based on solvent extraction. *Colloids Surf. A Physicochem. Eng. Asp.* **2023**, *670*, 131517. [CrossRef]
27. Zhang, W.; Cheng, C.Y. Manganese metallurgy review. Part I: Leaching of ores/secondary materials and recovery of electrolytic/chemical manganese dioxide. *Hydrometallurgy* **2007**, *89*, 137–159. [CrossRef]
28. Ma, X.; Tan, H.; He, X. Preparation and surface modification of anhydrous calcium sulfate whiskers from FGD gypsum in autoclave-free hydrothermal system. *Energy Sources Part A Recovery Util. Environ. Eff.* **2018**, *40*, 2055–2062. [CrossRef]
29. Fu, Y.; Qiao, H.; Feng, Q.; Chen, K.; Li, Y.; Xue, C.; Zhang, Y. Review of new methods for resource utilisation of electrolytic manganese residue and its application in building materials. *Constr. Build. Mater.* **2023**, *401*, 132901. [CrossRef]
30. He, Z.; Tang, L.; Chen, K.; Wang, X.; Shen, Z.; Xiao, Y. Study on the mechanism and mechanical properties of magnesium oxychloride cement for blocking pollutants migration from electrolytic manganese residue. *J. Mater. Cycles Waste Manag.* **2023**, *25*, 3161–3174. [CrossRef]
31. Ma, M.; Du, Y.; Bao, S.; Li, J.; Wei, H.; Lv, Y.; Song, X.; Zhang, T.; Du, D. Removal of cadmium and lead from aqueous solutions by thermal activated electrolytic manganese residues. *Sci. Total Environ.* **2020**, *748*, 141490. [CrossRef]
32. Deng, Y.; Shu, J.; Lei, T.; Zeng, X.; Li, B.; Chen, M. A green method for Mn^{2+} and NH^{4+}-N removal in electrolytic manganese residue leachate by electric field and phosphorus ore flotation tailings. *Sep. Purif. Technol.* **2021**, *270*, 118820. [CrossRef]
33. Shu, J.; Wu, H.; Liu, R.; Liu, Z.; Li, B.; Chen, M.; Tao, C. Simultaneous stabilization/solidification of Mn^{2+} and -NH^{4+}N from electrolytic manganese residue using MgO and different phosphate resource. *Ecotoxicol. Environ. Saf.* **2018**, *148*, 220–227. [CrossRef]
34. Zhou, Y. Reusing electrolytic manganese residue as an activator: The effect of calcination on its mineralogy and activity. *Constr. Build. Mater.* **2021**, *294*, 123533. [CrossRef]
35. Yao, L.; Xin, G.; Pu, P.; Yang, L.; Jiang, X.; Jiang, Z.; Jiang, W. Promotion of manganese extraction and flue gas desulfurization with manganese ore by iron in the anodic solution of electrolytic manganese. *Hydrometallurgy* **2021**, *199*, 105542. [CrossRef]
36. Jun, C.; Fukang, J.; Chengshan, H.; Qianxu, Y. Study on the adsorption performance of electrolytic manganese slag-based zeolite for manganese ions. *Inorg. Salt Ind.* **2020**, *51*, 61–66. [CrossRef]
37. Li, C.; Zhong, H.; Wang, S.; Xue, J. Leaching Behavior and Risk Assessment of Heavy Metals in a Landfill of Electrolytic Manganese Residue in Western Hunan, China. *Hum. Ecol. Risk Assess. Int. J.* **2014**, *20*, 1249–1263. [CrossRef]
38. Su, H.; Zhou, W.; Lyu, X.; Liu, X.; Gao, W.; Li, C.; Li, S. Remediation treatment and resource utilization trends of electrolytic manganese residue. *Miner. Eng.* **2023**, *202*, 108264. [CrossRef]
39. Li, W.; Jin, H.; Xie, H.; Wang, D. Progress in comprehensive utilization of electrolytic manganese residue: A review. *Environ. Sci. Pollut. Res.* **2023**, *30*, 48837–48853. [CrossRef]
40. Tsay, M.-Y. A bibliometric analysis of hydrogen energy literature, 1965–2005. *Scientometrics* **2008**, *75*, 421–438. [CrossRef]
41. Chen, H.; Jiang, W.; Yang, Y.; Yang, Y.; Man, X. Global trends of municipal solid waste research from 1997 to 2014 using bibliometric analysis. *J. Air Waste Manag. Assoc.* **2015**, *65*, 1161–1170. [CrossRef]
42. Borthakur, A.; Govind, M. Public understandings of E-waste and its disposal in urban India: From a review towards a conceptual framework. *J. Clean. Prod.* **2018**, *172*, 1053–1066. [CrossRef]

43. Duan, N.; Fan, W.; Changbo, Z.; Chunlei, Z.; Hongbing, Y. Analysis of pollution materials generated from electrolytic manganese industries in China. *Resour. Conserv. Recycl.* **2010**, *54*, 506–511. [CrossRef]
44. Shi, Y.; Long, G.; Wang, F.; Xie, Y.; Bai, M. Innovative co-treatment technology for effective disposal of electrolytic manganese residue. *Environ. Pollut.* **2023**, *335*, 122234. [CrossRef] [PubMed]
45. He, S.; Wilson, B.P.; Lundström, M.; Liu, Z. Hazard-free treatment of electrolytic manganese residue and recovery of manganese using low temperature roasting-water washing process. *J. Hazard. Mater.* **2021**, *402*, 123561. [CrossRef] [PubMed]
46. Lan, J.; Dong, Y.; Xiang, Y.; Zhang, S.; Mei, T.; Hou, H. Selective recovery of manganese from electrolytic manganese residue by using water as extractant under mechanochemical ball grinding: Mechanism and kinetics. *J. Hazard. Mater.* **2021**, *415*, 125556. [CrossRef]
47. Zheng, F.; Zhu, H.; Luo, T.; Wang, H.; Hou, H. Pure water leaching soluble manganese from electrolytic manganese residue: Leaching kinetics model analysis and characterization. *J. Environ. Chem. Eng.* **2020**, *8*, 103916. [CrossRef]
48. Chen, H.; Zhang, Y.; Zhang, Q.; Li, L. Technology conditions and kinetics analysis of manganese and iron ions leaching from electrolytic manganese residue by acid reduction. *Bull. Chin. Ceram. Soc.* **2017**, *36*, 2844–28849.
49. Yang, X.; Xiang, X.; Xue, X. Study on acid leaching experimental conditions of electrolytic manganese residue. *Bull. Chin. Ceram. Soc.* **2018**, *37*, 7.
50. Zou, Q.; Liu, H.; Xie, H. Leaching process of electrolytic manganese slag by alkali solution and its kinetics. *Miner. Metall. Eng.* **2018**, *38*, 83–87. (In Chinese) [CrossRef]
51. Li, C.; Zhong, H.; Wang, S.; Xue, J.; Zhang, Z. Removal of basic dye (methylene blue) from aqueous solution using zeolite synthesized from electrolytic manganese residue. *J. Ind. Eng. Chem.* **2015**, *23*, 344–352. [CrossRef]
52. Wang, N.; Fang, Z.; Peng, S.; Cheng, D.; Du, B.; Zhou, C. Recovery of soluble manganese from electrolyte manganese residue using a combination of ammonia and CO_2. *Hydrometallurgy* **2016**, *164*, 288–294. [CrossRef]
53. Shu, J.; Wu, Y.; Deng, Y.; Lei, T.; Huang, J.; Han, Y.; Zhang, X.; Zhao, Z.; Wei, Y.; Chen, M. Enhanced removal of Mn^{2+} and NH^{4+}-N in electrolytic manganese metal residue using washing and electrolytic oxidation. *Sep. Purif. Technol.* **2021**, *270*, 118798. [CrossRef]
54. Zhang, Y.; Cui, J.; Xu, C.; Yang, J.; Liu, M.; Ren, M.; Tan, X.; Lin, A.; Yang, W. The formation of discharge standards of pollutants for municipal wastewater treatment plants needs adapt to local conditions in China. *Environ. Sci. Pollut. Res.* **2023**, *30*, 57207–57211. [CrossRef]
55. Lai, H.; Huang, L.; Gan, C.; Xing, P.; Li, J.; Luo, X. Enhanced acid leaching of metallurgical grade silicon in hydrofluoric acid containing hydrogen peroxide as oxidizing agent. *Hydrometallurgy* **2016**, *164*, 103–110. [CrossRef]
56. Wu, S.; Wang, L.; Zhao, L.; Zhang, P.; El-Shall, H.; Moudgil, B.; Haung, X.; Zhang, L. Recovery of rare earth elements from phosphate rock by hydrometallurgical processes—A critical review. *Chem. Eng. J.* **2018**, *335*, 774–800. [CrossRef]
57. Yuzhu, O.; Youji, L.; Hui, L.; Zhiping, L.; Xiaowei, P.; Wenbin, Y. Recovery of manganese from electrolytic manganese residue by different leaching techniques in the presence of accessory ingredients. *Rare Met. Mater. Eng.* **2008**, *37*, 603–608.
58. Peng, T.; Xu, L.; Chen, H. Preparation and characterization of high specific surface area Mn_3O_4 from electrolytic manganese residue. *Cent. Eur. J. Chem.* **2010**, *8*, 1059–1068. [CrossRef]
59. Peng, T.; Xu, L.; Wang, X. Leaching of manganese residue for the preparation of trimanganese tetroxide with a high surface area. *Chin. J. Geochem.* **2013**, *32*, 331–336. [CrossRef]
60. Shu, J.; Lin, F.; Chen, M.; Li, B.; Wei, L.; Wang, J.; Luo, Z.; Wang, R. An innovative method to enhance manganese and ammonia nitrogen leaching from electrolytic manganese residue by surfactant and anode iron plate. *Hydrometallurgy* **2020**, *193*, 105311. [CrossRef]
61. Rao, S.; Sun, J.; Wang, D.; Liu, Z.; Zhu, W.; Cao, H.; Duan, L. Selective recovery of manganese and lead from electrolytic manganese residues in a sulfuric acid solution with galena as the reductant. *Sep. Purif. Technol.* **2023**, *308*, 122937. [CrossRef]
62. Wu, S.; Liu, R.; Liu, Z.; Du, J.; Tao, C. Electrokinetic remediation of electrolytic manganese residue using solar-cell and leachate-recirculation. *J. Chem. Eng. Jpn.* **2019**, *52*, 710–717. [CrossRef]
63. Zhao, Z.; Wang, R.; Shu, J.; Chen, M.; Xu, Z.; Han, Y.; Zhang, X.; Zhao, Z.; Wei, Y.; Chen, M. Enhanced manganese leaching from electrolytic manganese residue by electrochemical process and Na_2SO_3. *Miner. Eng.* **2022**, *189*, 107862. [CrossRef]
64. Shu, J.; Liu, R.; Liu, Z.; Chen, H.; Tao, C. Leaching of manganese from electrolytic manganese residue by electro-reduction. *Environ. Technol.* **2017**, *38*, 2077–2084. [CrossRef] [PubMed]
65. Shu, J.; Sun, X.; Liu, R.; Liu, Z.; Wu, H.; Chen, M.; Li, B. Enhanced electrokinetic remediation of manganese and ammonia nitrogen from electrolytic manganese residue using pulsed electric field in different enhancement agents. *Ecotoxicol. Environ. Saf.* **2019**, *171*, 523–529. [CrossRef] [PubMed]
66. Liu, R.; Wang, H.; Liu, Z.; Tao, C. Electrokinetic remediation with solar powered for electrolytic manganese residue and researching on migration of ammonia nitrogen and manganese. *J. Water Process Eng.* **2020**, *38*, 101655. [CrossRef]
67. Suanon, F.; Tang, L.; Sheng, H.; Fu, Y.; Xiang, L.; Herzberger, A.; Jiang, X.; Mama, D.; Wang, F. TW80 and GLDA-enhanced oxidation under electrokinetic remediation for aged contaminated-soil: Does it worth? *Chem. Eng. J.* **2020**, *385*, 123934. [CrossRef]
68. Yang, Y.; Shu, J.; Zhang, L.; Su, P.; Meng, W.; Wan, Q.; Liu, Z.; Liu, R.; Chen, F.; Ming, X. Enhanced Leaching of Mn from Electrolytic Manganese Anode Slime via an Electric Field. *Energy Fuels* **2021**, *35*, 20224–20230. [CrossRef]
69. Guo, X.; Yi, Y.; Shi, J.; Tian, Q. Leaching behavior of metals from high-arsenic dust by NaOH–Na_2S alkaline leaching. *Trans. Nonferrous Met. Soc. China* **2016**, *26*, 575–580. [CrossRef]

70. Shu, J.; Deng, Y.; Wei, X.; Chen, M.; Yang, Y.; Deng, Z. Migration and Transformation Behavior of Mn^{2+} and NH^{4+}-N in Electrolytic Manganese Residue at Different Leaching pH Environments: Release Kinetic Model, Physical Phase Changes, and Formation of Manganese Oxide. *ACS ES T Water* **2023**, *3*, 2229–2237. [CrossRef]
71. Zhou, C.; Wang, J.; Wang, N. Treating electrolytic manganese residue with alkaline additives for stabilizing manganese and removing ammonia. *Korean J. Chem. Eng.* **2013**, *30*, 2037–2042. [CrossRef]
72. Shu, J.; Liu, R.; Liu, Z.; Chen, H.; Du, J.; Tao, C. Solidification/stabilization of electrolytic manganese residue using phosphate resource and low-grade MgO/CaO. *J. Hazard. Mater.* **2016**, *317*, 267–274. [CrossRef]
73. Zhang, D.; Xiao, D.; Yu, Q.; Chen, S.; Chen, S.; Miao, M. Preparation of Mesoporous Silica from Electrolytic Manganese Slags by Using Amino-Ended Hyperbranched Polyamide as Template. *ACS Sustain. Chem. Eng.* **2017**, *5*, 10258–10265. [CrossRef]
74. Li, J.; Li, J.; Wei, H.; Yang, X.; Benoit, G.; Jiao, X. Alkaline-thermal activated electrolytic manganese residue-based geopolymers for efficient immobilization of heavy metals. *Constr. Build. Mater.* **2021**, *298*, 123853. [CrossRef]
75. Lan, J.; Sun, Y.; Guo, L.; Du, Y.; Du, D.; Zhang, T.; Li, J.; Ye, H. Highly efficient removal of As(V) with modified electrolytic manganese residues (M-EMRs) as a novel adsorbent. *J. Alloys. Compd.* **2019**, *811*, 151973. [CrossRef]
76. Liang, D.; Qin, F.; Li, X.; Jiang, J. Performance of Concrete Made with Manganese Slag. *Appl. Mech. Mater.* **2012**, *117*, 1185–1189. [CrossRef]
77. Zhao, S.; Zheng, W.; Wang, C.; He, F.; Wang, J.; Lin, X.; Luo, X.; Feng, J. Environmentally-friendly biorecovery of manganese from electrolytic manganese residue using a novel Penicillium oxalicum strain Z6-5-1: Kinetics and mechanism. *J. Hazard. Mater.* **2023**, *446*, 130662. [CrossRef]
78. Roy, J.J.; Madhavi, S.; Cao, B. Metal extraction from spent lithium-ion batteries (LIBs) at high pulp density by environmentally friendly bioleaching process. *J. Clean. Prod.* **2021**, *280*, 124242. [CrossRef]
79. Sur, I.M.; Micle, V.; Hegyi, A.; Lăzărescu, A.-V. Extraction of Metals from Polluted Soils by Bioleaching in Relation to Environmental Risk Assessment. *Materials* **2022**, *15*, 3973. [CrossRef]
80. Zhang, R.; Chen, R.; Nie, Y.; Xia, L.; Li, P.; Fan, X.; Zheng, L. Extraction of Al and rare earths (Ce, Gd, Sc, Y) from red mud by aerobic and anaerobic bi-stage bioleaching. *Chem. Eng. J.* **2020**, *401*, 125914. [CrossRef]
81. Lv, Y.; Li, J.; Ye, H.; Xu, Z.; Du, D.; Chen, S. Bioleaching of electrolytic manganese residue by silicate bacteria, and optimization of parameters during the leaching process. *Miner. Metall. Process.* **2018**, *35*, 176–183. [CrossRef]
82. Lv, Y.; Li, J.; Ye, H.; Du, D.; Li, J.; Sun, P.; Ma, M.; Wen, J. Bioleaching behaviors of silicon and metals in electrolytic manganese residue using silicate bacteria. *J. Clean. Prod.* **2019**, *228*, 901–909. [CrossRef]
83. Xin, B.; Chen, B.; Duan, N.; Zhou, C. Extraction of manganese from electrolytic manganese residue by bioleaching. *Bioresour. Technol.* **2011**, *102*, 1683–1687. [CrossRef] [PubMed]
84. Lv, Y.; Li, J.; Ye, H.; Du, D.; Gan, C.; Sun, P.; Wen, J. Bioleaching of silicon in electrolytic manganese residue using single and mixed silicate bacteria. *Bioprocess Biosyst. Eng.* **2019**, *42*, 1819–1828. [CrossRef] [PubMed]
85. Lv, Y.; Li, J.; Ye, H.; Du, D.; Sun, P.; Ma, M.; Zhang, T. Bioleaching of silicon in electrolytic manganese residue (EMR) by Paenibacillus mucilaginosus: Impact of silicate mineral structures. *Chemosphere* **2020**, *256*, 127043. [CrossRef] [PubMed]
86. Duan, N.; Zhou, C.; Chen, B.; Jiang, W.; Xin, B. Bioleaching of Mn from manganese residues by the mixed culture of Acidithiobacillus and mechanism. *J. Chem. Technol. Biotechnol.* **2011**, *86*, 832–837. [CrossRef]
87. Lan, J.; Sun, Y.; Chen, X.; Zhan, W.; Du, Y.; Zhang, T.; Ye, H.; Du, D.; Hou, H. Bio-leaching of manganese from electrolytic manganese slag by Microbacterium trichothecenolyticum Y1: Mechanism and characteristics of microbial metabolites. *Bioresour. Technol.* **2021**, *319*, 124056. [CrossRef]
88. Huang, L.; Li, X.; Hu, J.; Deng, Q.; Yang, C.; Liu, W.; Zhao, F.L.; Jiang, H. Recovery of manganese as spinel $MgMn_2O_4$ cathode material from electrolytic manganese residue by Na2CO3 hydrothermal-roasting process. *Sep. Purif. Technol.* **2024**, *336*, 126248. [CrossRef]
89. Zhang, L.; Xiong, Y.; Liu, H.; Li, Y.; Chen, S.; Tian, S. Hazard-Free Treatment of Electrolytic Manganese Residue and Recovery of High-Concentration SO_2 Using High-Temperature Reduction Roasting Process. *Separations* **2023**, *10*, 288. [CrossRef]
90. Li, G.; Liu, M.; Rao, M.; Jiang, T.; Zhuang, J.; Zhang, Y. Stepwise extraction of valuable components from red mud based on reductive roasting with sodium salts. *J. Hazard. Mater.* **2014**, *280*, 774–780. [CrossRef]
91. Li, J.; Du, D.; Peng, Q.; Wu, C.; Lv, K.; Ye, H.; Chen, S.; Zhan, W. Activation of silicon in the electrolytic manganese residue by mechanical grinding-roasting. *J. Clean. Prod.* **2018**, *192*, 347–353. [CrossRef]
92. Zhan, X.; Wang, J.; Yue, Z.; Deng, R.; Wang, Y.; Xu, X. Roasting mechanism of lightweight low-aluminum–silicon ceramisite derived from municipal solid waste incineration fly ash and electrolytic manganese residue. *Waste Manag.* **2022**, *153*, 264–274. [CrossRef]
93. Guo, X.; Qin, H.; Tian, Q.; Zhang, L. The efficacy of a new iodination roasting technology to recover gold and silver from refractory gold tailing. *J. Clean. Prod.* **2020**, *261*, 121147. [CrossRef]
94. Peng, N.; Pan, Q.; Liu, H.; Yang, Z.; Wang, G. Recovery of iron and manganese from iron-bearing manganese residues by multi-step roasting and magnetic separation. *Miner. Eng.* **2018**, *126*, 177–183. [CrossRef]
95. Sun, W.; Wang, Q.; Ding, S.; Su, S. Simultaneous absorption of SO_2 and NO_x with pyrolusite slurry combined with gas-phase oxidation of NO using ozone: Effect of molar ratio of $O_2/(SO_2 + 0.5NO_x)$ in flue gas. *Chem. Eng. J.* **2013**, *228*, 700–707. [CrossRef]

96. Huang, L.; Li, X.; Li, Q.; Wang, Q.; Zhao, F.; Liu, W. Ammonia removal and simultaneous immobilization of manganese and magnesium from electrolytic manganese residue by a low-temperature CaO roasting process. *Environ. Sci. Pollut. Res.* **2024**, *31*, 11321–11333. [CrossRef]
97. Li, X.; Zhou, M.; Chen, F.; Li, J.; Li, Y.; Wang, Y.; Hou, H. Clean Stepwise Extraction of Valuable Components from Electrolytic Manganese Residue via Reducing Leaching–Roasting. *ACS Sustain. Chem. Eng.* **2021**, *9*, 8069–8079. [CrossRef]
98. He, S.; Liu, Z. Efficient process for recovery of waste $LiMn_2O_4$ cathode material: Low-temperature $(NH^{4+})_2SO_4$ calcination mechanisms and water-leaching characteristics. *Waste Manag.* **2020**, *108*, 28–40. [CrossRef]
99. Nakajima, K.; Takeda, O.; Miki, T.; Matsubae, K.; Nagasaka, T. Thermodynamic Analysis for the Controllability of Elements in the Recycling Process of Metals. *Environ. Sci. Technol.* **2011**, *45*, 4929–4936. [CrossRef]
100. Xue, Y.; Yang, T.; Liu, X.; Cao, Z.; Gu, J.; Wang, Y. Enabling efficient and economical degradation of PCDD/Fs in MSWIFA via catalysis and dechlorination effect of EMR in synergistic thermal treatment. *Chemosphere* **2023**, *342*, 140164. [CrossRef]
101. He, W.L.; Li, R.; Yang, Y.P.; Zhang, Y.; Nie, D. Kinetic and thermodynamic analysis on preparation of belite-calcium sulphoaluminate cement using electrolytic manganese residue and barium slag by TGA. *Environ. Sci. Pollut. Res.* **2023**, *30*, 95901–95916. [CrossRef]
102. Huang, Y.; Zhang, Q. Highly Efficient Removal of Cu (II) with Modified Electrolytic Manganese Residue as A Novel Adsorbent. *Arab. J. Sci. Eng.* **2022**, *47*, 6577–6589. [CrossRef]
103. Li, C.; Yu, Y.; Li, Q.; Zhong, H.; Wang, S. Kinetics and equilibrium studies of phosphate removal from aqueous solution by calcium silicate hydrate synthesized from electrolytic manganese residue. *Adsorpt. Sci. Technol.* **2019**, *37*, 547–565. [CrossRef]
104. Demirel, Y. Thermodynamic Analysis. *Arab. J. Sci. Eng.* **2013**, *38*, 221–249. [CrossRef]
105. Duan, N.; Cui, K.; Zhu, C.; Jin, S. Study on phase evolution and promoting the pozzolanic activity of electrolytic manganese residue during calcination. *Environ. Res.* **2023**, *227*, 115774. [CrossRef]
106. Wu, C.; Gu, S.; Zhang, Q.; Bai, Y.; Li, M.; Yuan, Y.; Wang, H.; Liu, X.; Yuan, Y.; Zhu, N.; et al. Electrochemically activated spinel manganese oxide for rechargeable aqueous aluminum battery. *Nat. Commun.* **2019**, *10*, 73. [CrossRef] [PubMed]
107. Zhang, Y.; Wang, J.; Liu, B.; Huang, J.; Ye, J.; Li, Y.; Su, Z.; Wang, J. Extraction and Separation of Mn and Pb from Electrolytic Manganese Anodic Slime (EMAS) via SO_2 Roasting Followed by Acid Leaching Process. *JOM* **2020**, *72*, 925–932. [CrossRef]
108. Ma, G.; Liu, X.; Lv, Y.; Yan, X.; Zhu, X.; Zhang, M. A Research Progress on Stabilization/Solidification of Electrolytic Manganese Residue. *Environ. Sci. Eng.* **2023**, 57–72. [CrossRef]
109. Shua, J.; Liua, R.; Liua, Z.; Chena, H.; Taoa, C. Leaching of manganese from electrolytic manganese residue by electro-reduction method. *Environ. Technol.* **2024**, *45*, 1248. [CrossRef]
110. Ye, D.; Xu, Z.; Fu, Y.; Zhao, Y. Effects of electrolytic manganese residue (EMR) to co-sintering mechanism of ceramic aggregate. *Int. J. Appl. Ceram. Technol.* **2022**, *19*, 3017–3029. [CrossRef]
111. Du, B.; Zhou, C.; Duan, N. Recycling of electrolytic manganese solid waste in autoclaved bricks preparation in China. *J. Mater. Cycles Waste Manag.* **2014**, *16*, 258–269. [CrossRef]
112. He, W.; Li, R.; Zhang, Y.; Nie, D. Synergistic use of electrolytic manganese residue and barium slag to prepare belite- sulphoaluminate cement study. *Constr. Build. Mater.* **2022**, *326*, 126672. [CrossRef]
113. Wang, J.; Peng, B.; Chai, L.; Zhang, Q.; Liu, Q. Preparation of electrolytic manganese residue–ground granulated blastfurnace slag cement. *Powder Technol.* **2013**, *241*, 12–18. [CrossRef]
114. Wang, Y. Research of utilizing electrolytic manganese residue for cement mineralizer. *Concrete* **2010**, *8*, 90–93.
115. Li, Q.; Liu, Q.; Peng, B.; Chai, L.; Liu, H. Self-cleaning performance of TiO_2-coating cement materials prepared based on solidification/stabilization of electrolytic manganese residue. *Constr. Build. Mater.* **2016**, *106*, 236–242. [CrossRef]
116. Song, M.; Jie, Z.; Huan, Y.; Peng, Z.; Qingjie, Z. Investigation on sintering properties of electrolytic manganese residue-shale-coal ash raw compacts. *EBSCO* **2019**, *46*, 133.
117. Zhou, C.; Du, B.; Wang, N.; Chen, Z. Preparation and strength property of autoclaved bricks from electrolytic manganese residue. *J. Clean. Prod.* **2014**, *84*, 707–714. [CrossRef]
118. Wang, Y.; Gao, S.; Liu, X.; Tang, B.; Mukiza, E.; Zhang, N. Preparation of non-sintered permeable bricks using electrolytic manganese residue: Environmental and NH_3-N recovery benefits. *J. Hazard. Mater.* **2019**, *378*. [CrossRef]
119. Tang, B.; Gao, S.; Wang, Y.; Liu, X.; Zhang, N. Pore structure analysis of electrolytic manganese residue based permeable brick by using industrial CT. *Constr. Build. Mater.* **2019**, *208*, 697–709. [CrossRef]
120. Zhou, H.; Chen, P.; Zhao, Y.; Liu, R.; Wei, J. Sulfate activation of electrolytic manganese residue on heat-stewed steel slag activity. *Inorg. Chem. Ind.* **2019**, *51*, 66–69. Available online: https://www.scopus.com/inward/record.uri?eid=2-s2.0-85175825714&partnerID=40&md5=230e4012129c4dc5b10131645e25f41e (accessed on 10 May 2024).
121. Huang, C.; Shi, X.; Gong, J.; Chen, S. Alkali-activated electrolytic manganese residue preparation of cement admixture. *Chin. J. Environ. Eng.* **2017**, *11*, 1851–1856. [CrossRef]
122. Yang, C.; Lv, X.X.; Tian, X.K.; Wang, Y.X.; Komarneni, S. An investigation on the use of electrolytic manganese residue as filler in sulfur concrete. *Constr. Build. Mater.* **2014**, *73*, 305–310. [CrossRef]
123. Xu, Y.; Liu, X.; Zhang, Y.; Tang, B.; Mukiza, E. Investigation on sulfate activation of electrolytic manganese residue on early activity of blast furnace slag in cement-based cementitious material. *Constr. Build. Mater.* **2019**, *229*, 116831. [CrossRef]
124. Hou, P.-K.; Qian, J.-S.; Wang, Z.; Deng, C. Production of quasi-sulfoaluminate cementitious materials with electrolytic manganese residue. *Cem. Concr. Compos.* **2012**, *34*, 248–254. [CrossRef]

125. Wang, F.; Long, G.; Bai, M.; Shi, Y.; Zhou, J.L. Feasibility of low-carbon electrolytic manganese residue-based supplementary cementitious materials. *Sci. Total Environ.* **2023**, *883*, 163672. [CrossRef] [PubMed]
126. Liu, X.Y.; Ren, Y.Y.; Zhang, Z.Q.; Liu, X.M.; Wang, Y.G. Harmless treatment of electrolytic manganese residue: Ammonia nitrogen recovery, preparation of struvite and nonsintered bricks. *Chem. Eng. J.* **2023**, *455*, 140739. [CrossRef]
127. Li, J.; Lv, Y.; Jiao, X.; Sun, P.; Li, J.; Wuri, L. Zhang, T. Electrolytic manganese residue based autoclaved bricks with $Ca(OH)_2$ and thermal-mechanical activated K-feldspar additions. *Constr. Build. Mater.* **2020**, *230*, 116848. [CrossRef]
128. Lan, J.; Zhang, S.; Mei, T.; Dong, Y.; Hou, H. Mechanochemical modification of electrolytic manganese residue: Ammonium nitrogen recycling, heavy metal solidification, and baking-free brick preparation. *J. Clean. Prod.* **2021**, *329*, 129727. [CrossRef]
129. Wang, Y.; Ye, W.; Liu, H. The research on preparation of a new building material with EMR and their properties. *Adv. Mat. Res.* **2011**, *167–163*, 4575–4579. [CrossRef]
130. Wang, P.; Liu, D.-Y. Preparation of baking-free brick from manganese residue and its mechanical properties. *J. Nanomater.* **2013**, *2013*, 452854. [CrossRef]
131. Jiang, L. Heat treatment parameters of preparing glass-ceramic with electrolytic manganese residue and their properties. *J. Therm. Anal. Calorim.* **2020**, *140*, 1737–1744. [CrossRef]
132. Sławski, S.; Woźniak, A.; Bazan, P.; Mrówka, M. The Mechanical and Tribological Properties of Epoxy-Based Composites Filled with Manganese-Containing Waste. *Materials* **2022**, *15*, 1579. [CrossRef]
133. Qian, J.; Hou, P.; Wang, Z.; Qu, Y. Crystallization characteristic of glass-ceramic made from electrolytic manganese residue. *J. Wuhan Univ. Technol. Mater. Sci. Ed.* **2012**, *27*, 45–49. [CrossRef]
134. Wu, Y.; Shi, B.; Ge, W.; Yan, C.J.; Yang, X. Magnetic Separation and Magnetic Properties of Low-Grade Manganese Carbonate Ore. *JOM* **2014**, *67*, 361–368. [CrossRef]
135. Hu, C.; Wang, L.; Yang, L.; Bai, J. Optimization mixture ratio parameters of lightweight aggregates incorporating municipal solid waste incineration fly ash and electrolytic manganese residues using the Uniform Design Method. *Fresenius. Environ. Bull* **2018**, *27*, 9147–9155.
136. Hu, C.; Wang, L.; Zhan, X.; Gong, J.; Bai, J.; Yang, L. Preparation of ceramsite with MSWI fly ash and electrolytic manganese residues. *Chin. J. Environ. Eng.* **2019**, *13*, 177–185. [CrossRef]
137. Wu, J.; Song, M.; Xu, X.; Cheng, H.; Rao, Z. Prospects and advances of comprehensive utilization of electrolytic manganese residue. *Chin. J. Environ. Eng.* **2014**, *8*, 2645–2652.
138. Zhang, J.; Lian, Q.; Wang, J.; Chen, F. Experimental study on the preparation of ceramic wall and floor tiles with manganese residue. *China Ceram. Ind.* **2009**, *16*, 16–19.
139. Hu, C.; Yu, H. Preparation of ceramic bricks from electrolytic manganese residue. *Silic. Bull* **2010**, *29*, 112–115.
140. Cheng, H.; Ye, F.; Wei, H.; Shi, W.; Wu, S. Study on the effect of pore-forming agent on preparation of porous ceramics by electrolytic manganese slag. *Shandong Chem. Ind.* **2019**, *48*, 31. (In Chinese)
141. Zhan, X.; Wang, L.; Gong, J.; Wang, X.; Song, X.; Xu, T. Co-sintering MSWI fly ash with electrolytic manganese residue and coal fly ash for lightweight ceramisite. *Chemosphere* **2021**, *263*, 127914. [CrossRef]
142. An, X.; Wu, Z.; Qin, H.; Liu, X.; He, Y.; Xu, X.; Li, T.; Yu, B. Integrated co-pyrolysis and coating for the synthesis of a new coated biochar-based fertilizer with enhanced slow-release performance. *J. Clean. Prod.* **2021**, *283*, 124642. [CrossRef]
143. Lanzerstorfer, C. Potential of industrial de-dusting residues as a source of potassium for fertilizer production—A mini review. *Resour. Conserv. Recycl.* **2019**, *143*, 68–76. [CrossRef]
144. Mubula, Y.; Yu, M.; Yang, D.; Lin, B.; Guo, Y.; Qiu, T. Recovery of valuable elements from solid waste with the aid of external electric field: A review. *J. Environ. Chem. Eng.* **2023**, *11*, 111237. [CrossRef]
145. Das, N.; Jana, R.K. Adsorption of some bivalent heavy metal ions from aqueous solutions by manganese nodule leached residues. *J. Colloid Interface Sci.* **2006**, *293*, 253–262. [CrossRef] [PubMed]
146. Zhou, X.; Luo, C.; Wang, J.; Wang, H.; Chen, Z.; Wang, S.; Chen, Z. Recycling application of modified waste electrolytic manganese anode slag as efficient catalyst for PMS activation. *Sci. Total Environ.* **2021**, *762*, 143120. [CrossRef]
147. Jiang, M.; Du, Y.G.; Du, D.; Deng, Y.; Chen, N. Technology for producing silicon-manganese fertilizer from EMM residue. *China's Manganese Ind.* **2014**, *32*, 16–19.
148. Liu, T. Study on Preparation Technology of Electrolytic Manganese Residue Compound Fertilizer. Master's Thesis, Central South University, Changsha, China, 2012. (In Chinese).
149. Lv, Y.; Li, J.; Chen, Z.; Ye, H.; Du, D.; Shao, L.; Ma, M. Species identification and mutation breeding of silicon-activating bacteria isolated from electrolytic manganese residue. *Environ. Sci. Pollut. Res.* **2021**, *28*, 1491–1501. [CrossRef]
150. Xu, F.; Wang, X.; Chen, L.; Ding, D. Nutrition effect of Mn in manganese tailings on wheat growth. *Guizhou Agric. Sci.* **2010**, *8*, 56–58.
151. Zhang, Y.; Chen, Y.; Kang, W.; Han, H.; Song, H.; Zhang, C.; Wang, H.; Yang, X.; Gong, X.; Zhai, C.; et al. Excellent adsorption of Zn (II) using NaP zeolite adsorbent synthesized from coal fly ash via stage treatment. *J. Clean. Prod.* **2020**, *258*, 120736. [CrossRef]
152. Li, C.; Zhong, H.; Wang, S.; Xue, J.; Wu, F.; Zhang, Z. Manganese extraction by reduction–acid leaching from low-grade manganese oxide ores using CaS as reductant. *Trans. Nonferrous Met. Soc. China* **2015**, *25*, 1677–1684. [CrossRef]
153. Li, C.; Zhong, H.; Wang, S.; Xue, J.; Wu, F.; Zhang, Z. Preparation of MnO_2 and calcium silicate hydrate from electrolytic manganese residue and evaluation of adsorption properties. *J. Cent. South Univ.* **2015**, *22*, 2493–2502. [CrossRef]

154. Li, C.X.; Zhong, H.; Wang, S.; Xue, J.R.; Zhang, Z.Y. A novel conversion process for waste residue: Synthesis of zeolite from electrolytic manganese residue and its application to the removal of heavy metals. *Colloids Surf. A Physicochem. Eng. Asp.* **2015**, *470*, 258–267. [CrossRef]
155. Zhan, X.; Wang, L.; Wang, X.; Gong, J.; Yang, L.; Bai, J. Enhanced geopolymeric co-disposal efficiency of heavy metals from MSWI fly ash and electrolytic manganese residue using complex alkaline and calcining pre-treatment. *Waste Manag.* **2019**, *98*, 135–143. [CrossRef]
156. Zhao, R.; Han, F. Preparation of Geopolymer Using Electrolytic Manganese Residue. In *Key Engineering Materials*; Bao, Y., Jiang, D., Gong, J.H., Eds.; Trans Tech Publications Ltd.: Bäch, Switzerland, 2014; Volume 591, pp. 130–133. [CrossRef]
157. Li, J.; Sun, P.; Li, J.; Lv, Y.; Ye, H.; Shao, L.; Du, D. Synthesis of electrolytic manganese residue-fly ash based geopolymers with high compressive strength. *Constr. Build. Mater.* **2020**, *248*, 118489. [CrossRef]
158. Han, Y.C.; Cui, X.M.; Lv, X.S.; Wang, K.T. Preparation and characterization of geopolymers based on a phosphoric-acid-activated electrolytic manganese dioxide residue. *J. Clean. Prod.* **2018**, *205*, 488–498. [CrossRef]
159. Duan, H.; Hu, X.; Sun, Z. Magnetic zeolite imidazole framework material-8 as an effective and recyclable adsorbent for removal of ceftazidime from aqueous solution. *J. Hazard. Mater.* **2020**, *384*, 121406. [CrossRef]
160. Buaisha, M.; Balku, S.; Yaman, Ş.Ö. Heavy Metal Removal Investigation in Conventional Activated Sludge Systems. *Civ. Eng. J.* **2020**, *6*, 470–477. [CrossRef]
161. Hossain, N.; Bhuiyan, M.A.; Pramanik, B.K.; Nizamuddin, S.; Griffin, G. Waste materials for wastewater treatment and waste adsorbents for biofuel and cement supplement applications: A critical review. *J. Clean. Prod.* **2020**, *255*, 120261. [CrossRef]
162. Lan, J.; Sun, Y.; Huang, P.; Du, Y.; Zhan, W.; Zhang, T.; Du, D. Using Electrolytic Manganese Residue to prepare novel nanocomposite catalysts for efficient degradation of Azo Dyes in Fenton-like processes. *Chemosphere* **2020**, *252*, 126487. [CrossRef]
163. Li, M.; Huang, F.; Hu, L.; Sun, W.; Li, E.; Xiong, D.; Zhong, H.; He, Z. Efficient activation of peroxymonosulfate by a novel catalyst prepared directly from electrolytic manganese slag for degradation of recalcitrant organic pollutes. *Chem. Eng. J.* **2020**, *401*, 126085. [CrossRef]